An exact optimization model for the electric bus charging station location problem under inter-station travel time and energy consumption uncertainties

Dimitriadou, Androniki; Gkiotsalitis, Konstantinos; Liu, Tao; Cats, Oded

DOI
10.1016/j.trc.2025.105182

Publication date
2025

Document Version
Final published version

Published in
Transportation Research Part C: Emerging Technologies

Citation (APA)
Dimitriadou, A., Gkiotsalitis, K., Liu, T., & Cats, O. (2025). An exact optimization model for the electric bus charging station location problem under inter-station travel time and energy consumption uncertainties. *Transportation Research Part C: Emerging Technologies*, *178*, Article 105182. https://doi.org/10.1016/j.trc.2025.105182

Transportation Research Part C 178 (2025) 105182

Contents lists available at ScienceDirect

Transportation Research Part C

journal homepage: www.elsevier.com/locate/trc

An exact optimization model for the electric bus charging station location problem under inter-station travel time and energy consumption uncertainties

Androniki Dimitriadou [a], Konstantinos Gkiotsalitis [a,*], Tao Liu [b], Oded Cats [c]

[a] National Technical University of Athens, School of Civil Engineering, Department of Transportation Planning and Engineering, Zografou Campus, 9, Iroon Polytechniou str, 15773, Athens, Greece

[b] National Engineering Laboratory of Integrated Transportation Big Data Application Technology; National United Engineering Laboratory of Integrated and Intelligent Transportation, School of Transportation and Logistics, Southwest Jiaotong University, Chengdu 611756, China

[c] Delft University of Technology, Faculty of Civil Engineering and Geosciences, Building 23, Stevinweg 1, 2628 CN Delft, The Netherlands

ARTICLE INFO

Keywords:
Electric buses
Charging station location problem
Stochastic optimization
Minimum deadheading and queue waiting time
Travel time uncertainties
Energy consumption uncertainties

ABSTRACT

The shift towards environmentally friendly and efficient electric bus transportation systems oftentimes raises unexpected operational issues. This study models the Electric Bus Charging Station Location Problem (EB-CSLP) to develop a more resilient charging infrastructure, focusing on time-related and energy consumption uncertainties, specifically inter-station travel time delays. The model accommodates various charger types and maintains time continuity in the charging of electric buses. Initially formulated as a mixed-integer nonlinear program (MINLP), our stochastic optimization model is reformulated into a mixed-integer linear program (MILP) which minimizes both deadheading times and queue waiting times at the charging locations. The stochastic optimization model is tested in a real-world case study in Athens, Greece, considering multiple scenarios with varying inter-station travel times and energy consumption. The results demonstrate its effectiveness as a potential decision-support tool for selecting the optimal charger types and charging station locations under travel time and energy-related uncertainties.

1. Introduction

Globally, road transport emissions threaten urban air quality and contribute to global warming, primarily through the release of carbon dioxide (CO_2). The transport sector accounts for 24% of global air pollutants (International Energy Agency, 2024), 29% of U.S. greenhouse gas (GHG) emissions (U.S. Environmental Protection Agency, 2024), and 23.2% in the EU-28 (Eurostat, 2024), with carbon dioxide (CO_2), methane (CH_4), and nitrous oxide (N_2O) as the main pollutants (Shahid et al., 2014; Voigt et al., 2017). Reducing these emissions is vital for the sustainable development of transportation. The shift to electric buses is a key strategy, offering a cleaner public transport alternative (Lim et al., 2021; Shao et al., 2022).

To mitigate GHG emissions and combat global warming, numerous countries have announced carbon reduction plans. China aims for carbon neutrality by 2060 (Cheshmehzangi and Chen, 2021), and France has set a legislative goal to reach net-zero emissions by 2050 (Plessmann and Blechinger, 2017). As the transportation sector accounts for nearly one fourth of the global air pollutants and conventional diesel buses (DBs) emit harmful pollutants (PM, COx, NOx), replacing them with electric buses (EBs) is crucial. In

* Corresponding author.
E-mail address: kgkiotsalitis@civil.ntua.gr (K. Gkiotsalitis).

https://doi.org/10.1016/j.trc.2025.105182
Received 26 September 2024; Received in revised form 14 May 2025; Accepted 15 May 2025
Available online 18 June 2025

response, many European cities have committed to fully electrify bus fleets by 2030 (Elavarasan et al., 2022; Thorne et al., 2021). The U.S. government invested $7.5 billion in electric bus development, targeting a full transition by 2045 (Horrox and Casale, 2019), while Singapore and China have also made substantial progress with China maintaining over 90% of the global electric bus fleet (United Nations Economic and Social Commission for Asia and the Pacific (ESCAP), 2024; Cheshmehzangi and Chen, 2021).

The transition to electric buses requires new strategic planning (Teoh et al., 2017), especially in charging infrastructure development (Rigogiannis et al., 2023). Charging station placement is a strategic challenge (see the survey of Kchaou-Boujelben (2021)), preceding tactical-level decisions like frequency setting, timetabling, and vehicle scheduling (Gkiotsalitis, 2023; Gkiotsalitis et al., 2023b). Numerous studies have explored optimal charging infrastructure locations at depots (Uslu and Kaya, 2021; Hsu et al., 2021), en-route stops (Wu et al., 2021), and turnaround points (Randhahn and Knote, 2020), with the latter two enabling opportunity charging. While station-based static charging – typically conducted at bus depots and terminals – is cost-effective, opportunity charging at bus stops is a newly-adopted approach that can extend vehicle battery range and reduce deadhead mileage but may introduce charging conflicts and require costly fast-charging technologies (Wang et al., 2023).

The adoption of battery electric buses (BEBs) also introduces operational challenges, necessitating the mitigation of potential disruptions to ensure consistent functionality, reduced deadheading times, and minimized queue waiting costs. In the remainder of this paper, the *deadheading* term refers to the time electric buses travel without passengers from their final stop to a charging station, while *queue waiting time* denotes the delay an EB may experience between its arrival at the charging station and the start of the charging process (Gkiotsalitis, 2021). To minimize bus deadheading times and queue waiting costs under operational uncertainties, we optimize charging station locations, select suitable charger types, and schedule charging, while considering variability in the inter-station travel time and the energy consumption per traveled distance from when a bus finishes its trip until it reaches the charging station. Our model considers both slow and fast charging stations and variations in inter-station travel times and energy consumption during an operation day, providing valuable insights to policymakers and transportation authorities for *effective* and *resilient* strategic planning of the charging infrastructure's development.

The remainder of this paper is organized as follows. Section 2 reviews relevant EB-CSLP literature, covering both deterministic and stochastic approaches. Deterministic methods address the EB-CSLP without considering uncertainties, whereas stochastic methods incorporate uncertainty into the solution process. Section 3 presents the mathematical formulation of our model and its reformulation into a mixed-integer linear program. Section 4 expands on the model's formulation to include bus completion, deadheading and energy consumption uncertainties. Section 5 discusses experimental results and performance analysis based on a simplified transportation network using synthetic data as well as a real-world case study in the Athens metropolitan area. Finally, the concluding remarks section synthesizes the results and explores potential future research directions.

2. Literature review

This section offers a concise review of research focused on the optimal selection of charging stations, both deterministically and stochastically. It concludes by highlighting the existing knowledge gap that this study aims to address.

2.1. Electric bus charging station location problem without uncertainties

Traditional models for the Electric Bus Charging Station Location Problem (EB-CSLP) involve strategically placing charging infrastructure in bus networks to meet energy needs of electric buses while minimizing installation costs. Various mathematical models have been formulated to determine the best locations for charging stations across different configurations. Literature includes studies addressing the optimization of bus charging station locations with different goals.

Kunith et al. (2017) proposed a mixed-integer linear programming (MILP) optimization model to determine the minimum number and optimal layout of electric bus charging stations, as well as the appropriate battery capacity sizing, in order to minimize the total cost of ownership (TCO) and enable the feasible operation of buses in terms of energy consumption. Similarly, Lotfi et al. (2020) constructed a MILP model that can be applied to optimize the charging infrastructure configuration of various transport networks with different routes, electric bus models, and charger types, while minimizing the TCO. He et al. (2019) generated a MILP model for the optimal deployment of fast-charging stations in battery electric bus systems, taking into consideration the electricity demand of chargers and aiming to minimize the total cost of vehicle batteries, fast-charging stations, and energy storage systems. Uslu and Kaya (2021) developed a mixed-integer non-linear programming (MINLP) model to optimize the location and capacity of electric bus charging stations, minimizing waiting times and overall costs by placing charger at depots and terminals. Wu et al. (2021) introduced a model to optimize fast-charging station placement at established bus terminals, reducing system costs including infrastructure, energy, and bus waiting times.

In more recent years, Tzamakos et al. (2022) used an integer linear programming model to optimize fast wireless charger placement, minimizing investment costs and accounting bus queue delays with a M/M/1 queuing model. Meanwhile, Olsen and Kliewer (2022) integrated charging station placement with vehicle scheduling in public transport networks using a Variable Neighborhood Search metaheuristic solution method. Wang et al. (2023) focused on en-route fast charging infrastructure, optimizing placement and timing with MILP algorithms for efficient bus operations. He et al. (2023) developed a bi-objective integer linear model to create an optimal bus fleet transition plan. This plan includes selecting bus lines to add electric buses, the timing and type of battery electric buses to purchase, and deploying both en-route fast chargers and depot chargers. Finally, Basma et al. (2023) presented a two-step optimization algorithm that uses Dynamic Programming (DP) and GA to optimize battery sizing and charging strategies for electric bus fleets, specifically in Paris, improving the efficiency of the system and minimizing the TCO.

2.2. Electric bus charging station location and scheduling with uncertainties

In addition to deterministic charging station location problems, recent works have incorporated uncertainties into the decision-making process. Over the past few years, the optimization of the EB-CSLP for battery electric buses under uncertain conditions has received increasing attention in the literature.

A key starting point in this research area is the work of Liu et al. (2018), who planned fast-charging stations under energy consumption uncertainty using robust optimization. Their findings indicated that higher energy consumption uncertainty let to more conservative charging station placements, improving coverage but raising costs. An (2020) proposed a stochastic integer program to jointly optimize large-scale charging station locations and bus fleet size, incorporating random charging demand influenced by weather, traffic conditions, and time-of-use electricity tariffs. Utilizing the Sample Average Approximation (SAA) method and Lagrangian relaxation, they demonstrated that accounting for demand uncertainty improves network resilience by prioritizing charger placement in accessible locations rather than high-traffic areas. Hu et al. (2022) optimized en-route fast charger placement at bus stops, developing a deterministic model that considers penalty costs, variable electricity prices, and overlaps, then extending it with robust optimization to address uncertainties in passenger activity and travel times. Their findings highlighted the trade-off between bus delay minimization and energy sufficiency, favoring en-route fast charging in corridors with highly fluctuating passenger demand.

Expanding on EB-CSLP, additional studies have delved into the uncertainties associated with electric bus charging infrastructure planning. Deb et al. (2022) proposed a robust two-stage model for charging station placement, employing a Bayesian Network (BN) and a hybrid chicken swarm optimization algorithm with teaching-learning-based optimization (CSO-TLPO) to address road traffic variability. Their study highlighted that ignoring traffic uncertainty leads to suboptimal charger placement. Liu et al. (2022) introduced robust charging strategies for electric bus fleets, using column-generation-based approach (CG) to handle energy consumption uncertainties. Their results showed that uncertainty-aware charging schedules reduce the risk of electric bus battery depletion, especially during peak travel periods.

Zhou et al. (2023) proposed a two-stage stochastic model to deploy charging stations under uncertain travel times and battery degradation, using reinforcement learning (RL) and surrogate-based optimization (SBO). Their adaptive approach helped reduce costs and alleviate station congestion in networks with unpredictable traffic patterns. Finally, Esmaeilnejad et al. (2023) studied the impact of weather on electric-bus performance with a linear deterministic optimization model and a two-stage stochastic programming (SP) method, optimizing charging station locations and duration, while focusing on operational costs and weather effects. Their analysis revealed that temperature fluctuations significantly affect energy efficiency, increasing charging frequency and influencing charging station location decisions.

2.3. Study contribution

Several mathematical programming models have been developed for the EB-CSLP with and without uncertainties in recent years, varying in their decision variables and optimization objectives. While some have addressed specific uncertainties relevant to our research, such as inter-station travel time and energy-related parameters, their mathematical models were mainly solved using metaheuristics, potentially returning unstable and sub-optimal solutions that may vary across different model runs. Table 1 shows in detail the contribution of our study in relation to the state of the art, focusing on exact solution methodologies which return stable solutions.

In light of the past literature, our study addresses the EB-CSLP with multi-use charging stations located at existing bus depots, allowing for both slow and fast chargers rather than planning solely for fast chargers. As can be seen in Table 1, the majority of relevant models have not accounted for multi-use charging stations, as the charging infrastructure considered is primarily for en-route stations. Thus, the contributions of our work can be summarized as:

- development of a EB-CSLP model that accounts for multiple charger types (slow/fast), and its reformulation as an exact MILP, which can be solved to global optimality.
- incorporation of electric bus completion, deadheading time, and energy consumption uncertainties into the model's formulation, resulting in solutions that perform better under unfavorable conditions.
- testing and demonstration of the EB-CSLP model in a realistic bus network (Athens, Greece), considering different levels of variability.

3. Formulation as a minimum deadheading and queue waiting time problem

3.1. Mathematical program

In formulating this problem, we make the following key assumptions:

1. Each electric bus is considered fully charged before starting its operations on the specific line it serves.
2. Each electric bus is charged up to a sufficient level once the charging process is complete. This level depends on the time of day when the electric bus finishes its shift and requires charging.
3. Electric buses can be freely assigned to any charging location and type, if this is feasible in terms of battery autonomy.

Table 1
EB-CSLP summary of the most relevant literature.

Reference	Charging Location	Scheduling Decision	Multiple Charger Types	Optimization Goal	Uncertainties	Solution Approach
Liu et al. (2018)	Terminals, stops	Charging times		Implementation costs	Energy consumption	MILP
An (2020)	Depots, en-route	Charging times, bus fleet size		System costs	Charging demand	SAA and Heuristic (Lagrangian relaxation)
Uslu and Kaya (2021)	Terminals, depots, en-route	Charging stations capacity		Waiting times, overall costs		MINLP
Deb et al. (2022)	Terminal stops, depots	Charging scheduling		Costs, voltage stability, accessibility, waiting times	Road traffic	BN and Metaheuristic (CSO-TLPO)
Hu et al. (2022)	Stops	Charging scheduling		Infrastructure and penalty costs	Passengers' boarding, alighting times	MILP
Liu et al. (2022)	Depots, en-route	Charging scheduling	✓	Costs, energy shortages	Energy consumption	CG
Olsen and Kliewer (2022)	En-route	Charging, vehicle scheduling		Operational costs		Metaheuristic (VNS)
Basma et al. (2023)	En-route	Charging strategies, battery sizing		TCO		DP and Metaheuristic (GA)
Esmaeilnejad et al. (2023)	En-route	Charging locations, durations		Passengers' waiting time, capital costs	Weather conditions	Linear model and a two-stage SP model
Zhou et al. (2023)	Terminals, depots	Chargers: number and type	✓	Total costs	Travel times, battery degradation	Heuristic (RL and SBO)
This study	Depots, charging stations	Charging stations/types, vehicle assignment	✓	Deadheading and queue waiting time costs	Inter-station travel times and Energy consumption	MILP

4. There is no possibility for two or more vehicles to charge at the same charger simultaneously (chargers do not have multiple ports).
5. All electric buses follow the shortest route to their potential charging locations.

In our model, the predefined set $\mathcal{V}$ represents the potential physical locations for constructing charging stations. These physical locations can host up to $\mathcal{N}$ types of chargers, with the exact number depending on the outcome of our optimization problem, which takes into consideration the charging demand and the cost of deploying the chargers. The set $\mathcal{N}$ is divided into two subsets; $\mathcal{N}_1$ ($\subseteq \mathcal{N}$), representing slow chargers, and $\mathcal{N}_2$ ($\subseteq \mathcal{N}$), representing fast chargers. Any location in $\mathcal{V}$ can accommodate either type of charger, meaning $\mathcal{V} \subseteq \mathcal{N}$. Each charger $j \in \mathcal{N}$ can be used multiple times a day, as long as it serves only one bus at a time. In addition to the charger-related sets, a predetermined set $\mathcal{M}$ includes all electric buses, and from this, a subset $\mathcal{K} \subseteq \mathcal{M}$ indicates the buses requiring charging.

Taking into account the parameters of this problem, the state of charge for electric bus k, denoted as SOC_k, refers to the battery level of each bus after it has completed its operations and requires charging. It is generally assumed that SOC_k must remain within the predefined charging level boundaries ($SOC_k^{\min}$, $SOC_k^{\max}$) and reach a sufficient charge level (SOC_k^{suf}) upon completion of the charging process. This level depends on the time of the day when charging is required and is expressed as a percentage of $SOC_k^{\max}$, denoted as ω_k ($SOC_k^{suf} = \omega_k SOC_k^{\max}$). This percentage varies throughout the service day to minimize downtime and potential delays caused by charging, ensuring that buses can resume service in the shortest possible time. The time at which electric bus k reaches its final stop is represented by τ_k, while the deadheading time from the last stop of bus k to the potential charging location j is denoted by t_{kj}. We note that each electric bus k follows the minimum travel distance d_{kj} between its final stop and the potential

Table 2
Nomenclature.

Sets	
$\mathcal{V}$	set of all possible charging station physical locations
$\mathcal{N}$	set of all possible installation options for chargers, where $\mathcal{V} \subseteq \mathcal{N}$
$\mathcal{N}_1$	set of slow charger installation options
$\mathcal{N}_2$	set of fast charger installation options
$\mathcal{K}$	set of electric buses that need charging
Parameters	
SOC_k	state of charge of electric bus k after its completion at the final stop
$SOC_k^{\min}$	minimum allowed state of charge of electric bus k
$SOC_k^{\max}$	maximum allowed state of charge of electric bus k
SOC_k^{suf}	sufficient state of charge of electric bus k
ω_k	percentage for the definition of the sufficient state of charge of electric bus k
τ_k	time when electric bus k completes its shift at the last stop
M	a very large positive number
d_{kj}	minimum travel distance between the final stop of electric bus k and the potential charger location j
t_{kj}	estimated deadheading time from the last stop of electric bus k and the location of the potential charger j
e	battery consumption per traveled distance
$e^{\min}$	minimum battery consumption per traveled distance
$e^{\max}$	maximum battery consumption per traveled distance
b_j	fixed cost of installing a charger $j \in \mathcal{N}$
b^{max}	total amount of the installation budget
a_{kj}	indicator parameter that equals 1 if there exists a charger $j \in \mathcal{N}$ which is reachable from the last stop of electric bus k given its minimum state of charge, and 0 otherwise
r_1	slow charging rate
r_2	fast charging rate
λ_{1v}	maximum number of slow charging types at a charging station physical location $v \in \mathcal{V}$
λ_{2v}	maximum number of fast charging types at a charging station physical location $v \in \mathcal{V}$
c_l	end time of charging for all chargers each day
γ	parameter indicating the weight of bus deadheading time in relation to queue waiting time for charging
Variables	
$\mathbf{x}$	$\mathbf{x} = [x_1, \dots, x_j, \dots, x_{\lvert N \rvert}]^{\intercal}$, where $x_j = 1$ if we decide to construct the charger $j \in \mathcal{N}$, and $x_j = 0$ if not
q_{kj}	$q_{kj} \in \{0, 1\}$, where $q_{kj} = 1$ if the trip $k \in K$ is assigned to charger j, and 0 otherwise
f_{kj}	continuous variable, indicating the time when the bus k starts charging at charger j
l_{kj}	continuous variable, indicating the time when the bus k finishes charging at charger j
$\mathbf{y}$	$\mathbf{y} = [y_1, \dots, y_i, \dots, y_{\lvert K \rvert}]^{\intercal}$ deadheading time of electric bus $k \in \mathcal{K}$
$\mathbf{w}$	$\mathbf{w} = [w_1, \dots, w_i, \dots, w_{\lvert K \rvert}]^{\intercal}$ queue waiting time of electric bus $k \in \mathcal{K}$ from its arrival at the charger j until the start time of its charging

charging location. The charging need of every electric bus occurs after the respective bus completes a number of trips, which deplete its battery.

The battery consumption per unit distance, denoted by e, belongs within the electric bus energy consumption range ($e^{\min}$, $e^{\max}$), while the fixed cost of installing a charger $j \in \mathcal{N}$ is represented by b_j. The total budget available for charging station installations is b^{max}. Some additional charger-related parameters are r_1 and r_2, which denote the charging power of slow and fast charger types, respectively. Parameters λ_{1v} and λ_{2v} represent the maximum number of slow and fast charging types, accordingly, that a charging station physical location $v \in \mathcal{V}$ can accommodate. We also considered that chargers are available for use at any time throughout an operational day. The only constraint is a parameter c_l, which defines the closing time of the charging stations and indicates the latest time by which all the charging operations must be completed. The notations used in formulating this problem are listed in Table 2.

Considering the presented nomenclature, the mathematical model of the charging station location problem is presented below.

$(\tilde{Q})$:

$$\min \gamma \sum_{k \in \mathcal{K}} y_k + \sum_{k \in \mathcal{K}} w_k \tag{1}$$

s.t.:

$$y_k = \sum_{j \in N} t_{kj} q_{kj} \qquad \forall k \in K \tag{2}$$

$$w_k = \sum_{j \in N} [f_{kj} - (\tau_k + t_{kj})] q_{kj} \qquad \forall k \in K \tag{3}$$

$$\sum_{j\in\mathcal{N}} a_{kj}x_j \geq 1 \qquad \forall k \in \mathcal{K} \tag{4}$$

$$\sum_{j\in\mathcal{N}} q_{kj} = 1 \qquad \forall k \in \mathcal{K} \tag{5}$$

$$q_{kj} \leq x_j \qquad \forall k \in \mathcal{K}, \forall j \in \mathcal{N} \tag{6}$$

$$q_{kj} \leq a_{kj} \qquad \forall k \in \mathcal{K}, \forall j \in \mathcal{N} \tag{7}$$

$$\sum_{k\in\mathcal{K}} q_{kj} \geq x_j \qquad \forall j \in \mathcal{N} \tag{8}$$

$$\sum_{j\in\mathcal{N}_1} x_j \leq \lambda_{1v} \qquad \forall v \in \mathcal{V} \tag{9}$$

$$\sum_{j\in\mathcal{N}_2} x_j \leq \lambda_{2v} \qquad \forall v \in \mathcal{V} \tag{10}$$

$$\sum_{j\in\mathcal{N}} x_j b_j \leq b^{max} \tag{11}$$

$$f_{kj} \geq (\tau_k + t_{kj})q_{kj} \qquad \forall k \in \mathcal{K}, \forall j \in \mathcal{N} \tag{12}$$

$$l_{kj} \leq c_l q_{kj} \qquad \forall k \in \mathcal{K}, \forall j \in \mathcal{N} \tag{13}$$

$$l_{kj} = f_{kj} + q_{kj}\frac{\omega_k SOC_k^{\max} - (SOC_k - ed_{kj})}{r_1} \qquad \forall k \in \mathcal{K}, \forall j \in \mathcal{N}_1 \tag{14}$$

$$l_{kj} = f_{kj} + q_{kj}\frac{\omega_k SOC_k^{\max} - (SOC_k - ed_{kj})}{r_2} \qquad \forall k \in \mathcal{K}, \forall j \in \mathcal{N}_2 \tag{15}$$

$$SOC_k - eq_{kj}d_{kj} \geq SOC_k^{\min} \qquad \forall k \in \mathcal{K}, \forall j \in \mathcal{N} \tag{16}$$

$$q_{ij} + q_{kj} \leq 1 \text{ if } f_{ij} \leq f_{kj} \wedge f_{kj} < l_{ij} \qquad \forall k \in \mathcal{K}, \forall i \in \mathcal{K}\setminus\{k\}, \forall j \in \mathcal{N} \tag{17}$$

$$x_j \in \{0,1\} \qquad \forall k \in \mathcal{K} \tag{18}$$

$$q_{kj} \in \{0,1\} \qquad \forall k \in \mathcal{K}, \forall j \in \mathcal{N} \tag{19}$$

$$f_{kj}, l_{kj} \in \mathbb{R}_{\geq 0} \qquad \forall k \in \mathcal{K}, \forall j \in \mathcal{N} \tag{20}$$

$$y_k \in \mathbb{R}_{\geq 0} \qquad \forall k \in \mathcal{K} \tag{21}$$

$$w_k \in \mathbb{R}_{\geq 0} \qquad \forall k \in \mathcal{K} \tag{22}$$

The objective function (1) seeks to minimize the overall deadhead time and queue waiting time for charging. A weight γ is introduced in the objective function to emphasize the importance of minimizing the deadhead time for electric buses relative to the queue waiting time for charging. Minimizing deadheading time is critical because, during this period, the bus incurs high operational costs, including the driver's wages and the consumption of battery energy as the bus travels to the charging station. While queue waiting time is also significant, it does not contribute to operational costs in the same way, as, oftentimes, neither driver activity nor energy consumption is involved during this period. Constraints (2) define the deadheading time (t_{kj}) of each electric bus $k \in \mathcal{K}$ from its last stop to its charging location $j \in \mathcal{N}$. Constraints (3) define the queue waiting time for each bus k at charger j as the duration from its arrival at the charging location until the start time of its charging (f_{kj}). Constraints (4) ensure that each bus k has at least one charger j within reach. The accessibility requirement is enforced through the binary indicator parameter a_{kj}, which equals 1 if the electric bus's state of charge remains above the minimum threshold ($SOC_k^{\min}$) upon its arrival at the charger j, and 0 otherwise.

Constraints (5) guarantee that each bus k is assigned to exactly one charging location ($q_{kj} = 1$). Constraints (6) and (7) impose additional conditions, allowing a bus k to be assigned to charger j only if the charger is constructed ($x_j = 1$) and if it is reachable ($a_{kj} = 1$), respectively. Additionally, constraints (8) ensure that a charger j will only be constructed only if at least one bus k is assigned to it ($q_{kj} = 1$). Constraints (9) and (10) limit the number of charger types that each charging station location $v \in \mathcal{V}$ can accommodate, while constraints (11) ensure that the total installation cost of all chargers remain within the total budget, b^{max}. Constraints (12) regulate the charging sequence, ensuring that bus k starts charging at the assigned charger j only after arriving at it. Constraints (13) ensure that bus k completes its charging process at charger j (l_{kj}), if assigned to it, no later than the predefined charging end time c_l, which remains consistent across all chargers.

Constraints (14) and (15) calculate the time when bus k stops charging at charger j (l_{kj}), which equals the charging start time (f_{kj}) summed with the time needed to sufficiently charge the battery. Constraints (14) apply to electric buses assigned to a slow charging type ($j \in \mathcal{N}_1$), while constraints (15) apply to bus assigned to fast charging ($j \in \mathcal{N}_2$). The time required for bus k to charge up to a sufficient level is determined by the difference between the percentage of the maximum level of charge ($\omega_k SOC_k^{\max}$) that can be reached and its remaining battery level upon arriving at charger j, divided by the charger's charging rate (r_1 or r_2). The remaining battery level of bus k equals its state of charge when it is finished (SOC_k) minus the energy required to travel to charger j (ed_{kj}). In this model, the recharging duration is precisely calculated and depends on the bus remaining battery level and the charging rate of the assigned charger type (slow/fast). Constraints (16) ensure that the remaining battery level of bus k at the charger j, if assigned to it, remains above $SOC_k^{\min}$.

Charger $j \in \mathcal{N}$ can be used multiple times per day without predefined charging time slots. Consequently, the charging start time of each bus $k \in \mathcal{K}$ at charger j (f_{kj}) can take any positive continuous value at any charger. This flexibility raises the concern that the charging processes of multiple electric buses might overlap for a given charger. To prevent this, constraints (17) ensure that no charger can be used by more than one vehicle at the same time. In more detail, if bus $i \in \mathcal{K} \setminus \{k\}$ is assigned to charger j and starts charging before another bus k ($f_{ij} \leq f_{kj}$), bus k cannot be assigned to charger j if the start time of its charging (f_{kj}) precedes the end time of the charging of bus i (l_{ij}). That is, $q_{ij} + q_{kj} \leq 1$ if $f_{ij} \leq f_{kj}$ and $f_{kj} < l_{ij}$.

In some of the aforementioned constraints, the big-M approach was utilized. This involved setting M as a large positive number ($M \ggg 0$), greater than the relevant terms in the constraints, to ensure their enforcement or relaxation as needed.

3.2. Linearizations

Mathematical program ($\tilde{Q}$) is non-convex because of the nonlinear constraints (3) and constraints (17), which contain a logical expression. In constraints (3), nonlinearity arises due to the multiplication of the variables f_{kj} and q_{kj}. To address this, we reformulate w_k as follows (23) and we introduce the inequality constraints (24). Constraints (24) ensure that when the assignment of bus $k \in \mathcal{K}$ to a potential charger $j \in \mathcal{N}$ does not take place ($q_{kj} = 0$), the respective charging start time variable f_{kj} will automatically be set to 0.

$$w_k = \sum_{j \in \mathcal{N}} f_{kj} - (\tau_k + t_{kj}) q_{kj} \qquad \forall k \in \mathcal{K} \tag{23}$$

$$f_{kj} \leq M q_{kj} \qquad \forall k \in \mathcal{K}, \forall j \in \mathcal{N} \tag{24}$$

Considering constraints (17), we divided them into three distinct parts through constraints (25)–(30), introducing the binary variables d_{kij}, g_{kij}, h_{kij}, and the very small positive number ϵ.

Theorem 3.1. *Constraints (17): $q_{ij} + q_{kj} \leq 1$ if $f_{ij} \leq f_{kj}$ and $f_{kj} < l_{ij}$ $\forall k \in \mathcal{K}, \forall i \in \mathcal{K} \setminus \{k\}, \forall j \in \mathcal{N}$ and the following set of constraints are equisatisfiable:*

$$f_{ij} \leq f_{kj} + M(1 - d_{kij}) \qquad \forall k \in \mathcal{K}, \forall i \in \mathcal{K} \setminus \{k\}, \forall j \in \mathcal{N} \tag{25}$$

$$f_{ij} \geq f_{kj} + \epsilon - M d_{kij} \qquad \forall k \in \mathcal{K}, \forall i \in \mathcal{K} \setminus \{k\}, \forall j \in \mathcal{N} \tag{26}$$

$$f_{kj} \leq l_{ij} - \epsilon + M(1 - g_{kij}) \qquad \forall k \in \mathcal{K}, \forall i \in \mathcal{K} \setminus \{k\}, \forall j \in \mathcal{N} \tag{27}$$

$$f_{kj} \geq l_{ij} - M g_{kij} \qquad \forall k \in \mathcal{K}, \forall i \in \mathcal{K} \setminus \{k\}, \forall j \in \mathcal{N} \tag{28}$$

$$h_{kij} = \min(d_{kij}, g_{kij}) \qquad \forall k \in \mathcal{K}, \forall i \in \mathcal{K} \setminus \{k\}, \forall j \in \mathcal{N} \tag{29}$$

$$q_{ij} + q_{kj} \leq 1 + M(1 - h_{kij}) \qquad \forall k \in \mathcal{K}, \forall i \in \mathcal{K} \setminus \{k\}, \forall j \in \mathcal{N} \tag{30}$$

Proof. The first inequality part, $f_{ij} \leq f_{kj}$, in the logical expression of constraints (17) is replaced by constraints (25)–(26). These constraints ensure that the binary variable d_{kij} equals 1 if bus k starts charging at the same time as, or immediately after, the start time of charging of bus $i \in \mathcal{K} \setminus \{k\}$ at the charger j, and 0 otherwise. The small positive ϵ number is used to replace the greater sign ($>$) with the greater than or equal sign ($\geq$) in constraints (26). The second inequality part, $f_{kj} < l_{ij}$, in the logical expression of constraints (17) is replaced by constraints (27)–(28), which ensure that the binary variable g_{kij} equals 1 if bus k starts charging before bus i completes its charging at the charger j, and 0 otherwise. Note that the small positive ϵ value is used to interpret the less sign ($<$) of the second inequality part in the logical expression of constraints (17) with the less than or equal sign ($\leq$) through the constraints (27). The final part of constraints (17), expressed through the inequality $q_{ij} + q_{kj} \leq 1$, is replaced by constraints (29)–(30). Constraints (29) ensure that the binary variable h_{kij} receives the minimum value of d_{kij} and g_{kij}, so that when it equals 1, electric buses k and i are not assigned to the same charger j through constraints (30); otherwise it equals 0. ■

Finally, constraints (29) are also nonlinear. To address this, we introduce an additional binary variable z_{kij} to replace the nonlinear constraints (29) with the following linear (31)–(34).

$$h_{kij} \leq d_{kij} \qquad \forall k \in \mathcal{K}, \forall i \in \mathcal{K} \setminus \{k\}, \forall j \in \mathcal{N} \tag{31}$$

$$h_{kij} \leq g_{kij} \qquad \forall k \in \mathcal{K}, \forall i \in \mathcal{K} \setminus \{k\}, \forall j \in \mathcal{N} \tag{32}$$

$$h_{kij} \geq d_{kij} - M z_{kij} \qquad \forall k \in \mathcal{K}, \forall i \in \mathcal{K} \setminus \{k\}, \forall j \in \mathcal{N} \tag{33}$$

$$h_{kij} \geq g_{kij} + M(z_{kij} - 1) \qquad \forall k \in \mathcal{K}, \forall i \in \mathcal{K} \setminus \{k\}, \forall j \in \mathcal{N} \tag{34}$$

Note that constraints (31)–(34) and (29) are equisatisfiable. Thus, we can formulate ($\tilde{Q}$) as the following mixed-integer linear program ($\hat{Q}$):

($\hat{Q}$) :

$$\min \ \gamma \sum_{k \in \mathcal{K}} y_k + \sum_{k \in \mathcal{K}} w_k \tag{35}$$

s.t.: Equations (2), (4)–(16), (18)–(28), (30)–(34). (36)

Theorem 3.2. *Given that the problem is feasible, the continuous relaxation of the mathematical program ($\hat{Q}$) possesses a globally optimal solution.*

Proof. Mathematical program ($\hat{Q}$) in Eqs. (2), (4)–(16), (18)–(28), (30)–(34) is a mixed-integer linear program. The continuous relaxation of this program generates a feasible region composed of affine equality and inequality functions, forming a polyhedron. Since the objective function is linear, the continuous relaxation of the problem is both convex and concave. As a result, any locally optimal solution for the continuously relaxed problem constitutes also a globally optimal solution. ■

It follows from Theorem 3.2 that one can solve the mixed-integer linear program ($\hat{Q}$) to global optimality by using an exact method for mixed-integer linear programming, such as the Branch-and-Cut approach.

4. Charging station location selection problem under inter-station travel time and energy consumption uncertainties

During daily operations, electric buses can exhibit variability in their inter-station travel times and the time required to reach their assigned charging stations. Additionally, energy variability can also arise during the trip to the charging station, particularly in terms of battery consumption per unit of traveled distance. Numerous factors, such as traffic conditions and incidents, road works, extreme weather events, and in-vehicle passenger occupancy, can disrupt their operations. Therefore, it is crucial to incorporate the effects of these variabilities to our decision making. In the remainder of this section, we consider the following uncertainties for each electric bus $k \in \mathcal{K}$: (i) variability in the completion time, τ_k, (ii) variability in the deadheading time from the last stop to the potential charger location $j \in \mathcal{N}$, t_{kj}, and (iii) variability in the energy battery consumption per traveled distance, e, from the last stop to the potential charger j. To do so, parameters τ_k, t_{kj}, and e are now treated as uncertain - random parameters. A commonly used approach to handle uncertainties is to find a solution that optimizes the expected value of the objective function. Generally, this approach necessitates knowledge of the probability distributions of the random parameters (in our case: bus completion times, deadheading times, and energy battery consumption). Specifically, we aim to minimize the following objective function:

$$\mathbb{E}\left[\gamma \sum_{k\in\mathcal{K}} y_k + \sum_{k\in\mathcal{K}} w_k\right] \tag{37}$$

which can be equivalently written as:

$$\gamma \sum_{k\in\mathcal{K}} \sum_{j\in\mathcal{N}} \mathbb{E}[t_{kj}]q_{kj} + \sum_{k\in\mathcal{K}} \sum_{j\in\mathcal{N}} f_{kj} - \mathbb{E}[(\tau_k + t_{kj})]q_{kj} \tag{38}$$

where τ_k and t_{kj} are the *uncertain parameters* that are drawn from probability distributions. To solve this Stochastic Optimization Problem, we employ the Sample Average Approximation (SAA) method (Kim et al., 2015; Gkiotsalitis et al., 2022), which utilizes a random sample of the uncertain time parameters $\tau_{1,k}, \tau_{2,k}, \ldots, \tau_{|S|,k}$ and $t_{1,kj}, t_{2,kj}, \ldots, t_{|S|,kj}$ – where S is the set of travel times scenarios that are sampled from probability distributions of τ_k and t_{kj}, respectively. This approximates the value of the objective function expressed in (38), which can now be written as:

$$\frac{1}{|S|}\left[\gamma \sum_{s\in S}\sum_{k\in\mathcal{K}}\sum_{j\in\mathcal{N}} t_{s,kj}q_{kj} + \sum_{s\in S}\sum_{k\in\mathcal{K}}\sum_{j\in\mathcal{N}} f_{kj} - (\tau_{s,k} + t_{s,kj})q_{kj}\right] \tag{39}$$

Incorporating the time and energy-uncertain parameters $\tau_{s,k}$, $t_{s,kj}$, and e_s into the constraints of the optimization problem can lead to infeasibilities due to excessive completion times of buses $k \in \mathcal{K}$ at their final stops, as well as excessive deadheading times and energy consumption per traveled distance from their final stops to the potential charging locations $j \in \mathcal{N}$. This issue occurs from the time-related uncertainties, when the start time of charging for bus k at charger j (f_{kj}) is required to accommodate its constraints across all possible scenarios, including the outlier ones with unexpected delays. Energy consumption-related uncertainties can similarly lead to infeasibility when the state of charge of each bus k upon arrival at the potential charging location, and the charging end time at charger j (l_{kj}), must satisfy their constraints across all the scenarios, even in cases where battery energy consumption reaches high limits.

Therefore, constraints (12), which require the variable f_{kj} of bus $k \in \mathcal{K}$ to the charger $j \in \mathcal{N}$ to be greater than or equal to the sum of τ_k and t_{kj} ($f_{kj} \geq (\tau_k + t_{kj})q_{kj}$), can be relaxed to permit a small number of electric buses k to remain uncharged in scenarios with unexpectedly late completion and deadheading times. Similarly, constraints (14) and (15), which define the charging end time variable l_{kj} of bus k at charger j as the sum of its charging start time f_{kj} and the required charging duration for the sufficient charging of the electric bus, can be relaxed to allow a small number of electric buses k to undergo an incomplete charging process in scenarios with unexpectedly high energy consumption. Likewise, constraints (16), which ensure that the remaining state of charge of bus k at charger j stays above $SOC_k^{\min}$, can also be relaxed, allowing the state of charge of a limited number of electric buses k to fall below the minimum energy threshold. With these considerations, our optimization model ($\hat{Q}$), which incorporates the realizations of these uncertain elements, is formulated as follows:

$$(\hat{Q}):$$

$$\min \frac{1}{|S|}\left[\gamma \sum_{s\in S}\sum_{k\in\mathcal{K}}\sum_{j\in\mathcal{N}} t_{s,kj}q_{kj} + \sum_{s\in S}\sum_{k\in\mathcal{K}}\sum_{j\in\mathcal{N}} f_{kj} - (\tau_{s,k} + t_{s,kj})q_{kj}\right] \tag{40}$$

s.t.: Equations (4)–(11), (13), (18)–(22), (24)–(28), (30)–(34) (41)

$$C_{s,kj} = f_{kj} - (\tau_{s,k} + t_{s,kj})q_{kj} \qquad \forall k \in \mathcal{K}, \forall j \in \mathcal{N}, \forall s \in \{1, ..., S\} \tag{42}$$

$$\sum_{s \in S} \Pr\left(C_{s,kj} \geq 0\right) \geq \beta |S| \qquad \forall k \in \mathcal{K}, \forall j \in \mathcal{N} \tag{43}$$

$$C_{1,s,kj} = l_{kj} - f_{kj} - q_{kj} \frac{\omega_k SOC_k^{\max} - (SOC_k - e_s d_{kj})}{r_1} \qquad \forall k \in \mathcal{K}, \forall j \in \mathcal{N}_1, \forall s \in \{1, ..., S\} \tag{44}$$

$$C_{1,s,kj} = l_{kj} - f_{kj} - q_{kj} \frac{\omega_k SOC_k^{\max} - (SOC_k - e_s d_{kj})}{r_2} \qquad \forall k \in \mathcal{K}, \forall j \in \mathcal{N}_2, \forall s \in \{1, ..., S\} \tag{45}$$

$$\sum_{s \in S} \Pr\left(C_{1,s,kj} \geq 0\right) \geq \beta |S| \qquad \forall k \in \mathcal{K}, \forall j \in \mathcal{N} \tag{46}$$

$$C_{2,s,kj} = SOC_k - e_s q_{kj} d_{kj} - SOC_k^{\min} \qquad \forall k \in \mathcal{K}, \forall j \in \mathcal{N}, \forall s \in \{1, ..., S\} \tag{47}$$

$$\sum_{s \in S} \Pr\left(C_{2,s,kj} \geq 0\right) \geq \beta |S| \qquad \forall k \in \mathcal{K}, \forall j \in \mathcal{N} \tag{48}$$

$$C_{s,kj}, C_{1,s,kj}, C_{2,s,kj} \in \mathbb{R} \qquad \forall k \in \mathcal{K}, \forall j \in \mathcal{N}, \forall s \in \{1, ..., S\} \tag{49}$$

$$\beta \in (0, 1] \tag{50}$$

where constraints (42)–(50) modify the problem's formulation compared to its deterministic counterpart, substituting constraints (12) to account for inter-station travel time uncertainties and constraints (14)–(16) to address inter-station energy consumption variabilities. Constraints (42) introduce the variable $C_{s,kj}$, which computes the difference between f_{kj} and $(\tau_{s,k} + t_{s,kj})q_{kj}$ for each electric bus-charging station combination (k, j), and constraints (43) require the sum of the probabilities of $C_{s,kj} \geq 0$ across all scenarios $s \in S$ to reach or exceed a percentage β of the total number of uncertain scenarios $|S|$. Similarly, constraints (44) and (45) introduce the variable $C_{1,s,kj}$, which applies to both slow and fast chargers. This variable computes the difference between l_{kj} and f_{kj}, summed with the required charging duration for the sufficient charging of the bus, $\omega_k SOC_k^{\max}$, from its remaining battery level upon its arrival at the charging station. The remaining battery level of an electric bus $k \in \mathcal{K}$ at charger $j \in \mathcal{N}$ is defined as the charge level after its shift completion, SOC_k, minus the energy consumed traveling to charger j, $e_s d_{kj}$. Constraints (46) ensure that the sum of the probabilities of $C_{1,s,kj} \geq 0$ across all scenarios $s \in S$ meets or exceeds the $\beta(\%)$ of the total number of uncertain scenarios $|S|$. Constraints (47) introduce the variable $C_{2,s,kj}$, which computes the difference between the remaining battery level of an electric bus upon reaching charging station j and the $SOC_k^{\min}$. Like constraints (43) and (46), constraints (48) require the sum of probabilities of $C_{2,s,kj} \geq 0$ across all scenarios $s \in S$ to reach or exceed $\beta|S|$. This percentage β remains consistent across constraints (43), (46), and (48).

In more detail, constraints (43), (46), and (48) present the satisfaction probability of the stochastic expressions ($C_{s,kj} \geq 0$, $C_{1,s,kj} \geq 0$, $C_{2,s,kj} \geq 0$) holding true in no less than $\beta(\%)$ of all scenarios. When β equals 1, constraints (43), (46), and (48) become *stochastic constraints*, since they are forced to be satisfied in every scenario $s \in S$. This is because stochastic constraints demand a feasible decision to remain valid regardless of how uncertainty unfolds. Given the infeasibility that may arise from these strict requirements, an alternative approach is to relax the constraints, ensuring they hold true most of the time rather than always. In such a case, one tolerates the fact that for certain observed values of the uncertain parameters, the stochastic expressions $C_{s,kj} \geq 0$, $C_{1,s,kj} \geq 0$, and $C_{2,s,kj} \geq 0$ may not hold, but expects them to hold for at least a portion $\beta(\%)$ of the total number of scenarios. In this way, constraints (43), (46), and (48) transform into *chance constraints*, which are frequently used for uncertain combinatorial problems and belong to the broader realm of Stochastic Constraint Satisfaction Problems (SCSPs) (Zghidi et al., 2018). In these problems, uncertainty is modeled using random parameters to represent unpredictable factors, which can be sampled from various distributions, each with an associated probability.

4.1. Reformulation of the satisfaction probabilities and the objective function

To apply the satisfaction probability functions (43), (46), and (48), we reformulated them through constraints (51)–(59), introducing the binary variables $m_{s,kj}$, $o_{s,kj}$ and $\psi_{s,kj}$. The variable $m_{s,kj}$ takes the value of 1 when $C_{s,kj} \geq 0$, and 0 otherwise, counting in how many scenarios this stochastic expression holds. Similarly, $o_{s,kj}$ and $\psi_{s,kj}$ equal 1 when $C_{1,s,kj} \geq 0$ and $C_{2,s,kj} \geq 0$, respectively, and 0 otherwise.

$$C_{s,kj} \geq -M(1 - m_{s,kj}) \qquad \forall k \in \mathcal{K}, \forall j \in \mathcal{N}, \forall s \in \{1, \ldots, S\} \tag{51}$$

$$C_{s,kj} \leq -\epsilon + M m_{s,kj} \qquad \forall k \in \mathcal{K}, \forall j \in \mathcal{N}, \forall s \in \{1, \ldots, S\} \tag{52}$$

$$\sum_{s \in S} m_{s,kj} \geq \beta |S| \qquad \forall k \in \mathcal{K}, \forall j \in \mathcal{N} \tag{53}$$

$$C_{1,s,kj} \geq -M(1 - o_{s,kj}) \qquad \forall k \in \mathcal{K}, \forall j \in \mathcal{N}, \forall s \in \{1, \ldots, S\} \tag{54}$$

$$C_{1,s,kj} \leq -\epsilon + M o_{s,kj} \qquad \forall k \in \mathcal{K}, \forall j \in \mathcal{N}, \forall s \in \{1, \ldots, S\} \tag{55}$$

$$\sum_{s\in S} o_{s,kj} \geq \beta|S| \qquad \forall k \in \mathcal{K}, \forall j \in \mathcal{N} \tag{56}$$

$$C_{2,s,kj} \geq -M(1-\psi_{s,kj}) \qquad \forall k \in \mathcal{K}, \forall j \in \mathcal{N}, \forall s \in \{1,\ldots,S\} \tag{57}$$

$$C_{2,s,kj} \leq -\epsilon + M\psi_{s,kj} \qquad \forall k \in \mathcal{K}, \forall j \in \mathcal{N}, \forall s \in \{1,\ldots,S\} \tag{58}$$

$$\sum_{s\in S} \psi_{s,kj} \geq \beta|S| \qquad \forall k \in \mathcal{K}, \forall j \in \mathcal{N} \tag{59}$$

Constraints (53), (56), and (59) count the number of times $C_{s,kj}$, $C_{1,s,kj}$, and $C_{2,s,kj}$ are greater than or equal to 0 and compare these counts to the number of scenarios $\beta|S|$ that allow them to take negative values. Additionally, when we apply the satisfaction probability function (43) with $\beta < 1$, the variable $C_{s,kj}$ is allowed to fall below zero in a certain percentage of scenarios $s \in S$. Since $C_{s,kj}$ is also part of the objective function (40), we constrain the second part of the objective function – namely, the queue waiting time variable – to consider only non-negative values. The reformulated expression of the objective function can be written as follows:

$$(\hat{Q}):$$

$$\min \frac{1}{|S|}\left[\gamma \sum_{s\in S}\sum_{k\in\mathcal{K}}\sum_{j\in\mathcal{N}} t_{s,kj}q_{kj} + \sum_{s\in S}\sum_{k\in\mathcal{K}}\sum_{j\in\mathcal{N}} \max\left\{f_{kj} - (\tau_{s,k}+t_{s,kj})q_{kj}, 0\right\}\right] \tag{60}$$

Note that the second part of the objective function is nonlinear because it includes a maximization term. This can be linearized by inserting the continuous variable $\tilde{w}_{s,k} \in \mathbb{R}_{\geq 0}$ and using the following constraints (61)–(62).

$$\tilde{w}_{s,k} = \sum_{j\in N} f_{kj} - (\tau_{s,k}+t_{s,kj})q_{kj} \qquad \forall k \in K, \forall s \in S \tag{61}$$

$$\tilde{w}_{s,k} \geq 0 \qquad \forall k \in K, \forall s \in S \tag{62}$$

The newly inserted continuous variable $\tilde{w}_{s,k}$ replaces the nonlinear term

$$\max\left\{f_{kj} - (\tau_{s,k}+t_{s,kj})q_{kj}, 0\right\}$$

in the objective function, resulting in a mixed-integer linear program. Thus, the charging station location selection problem, considering inter-station travel time and energy consumption uncertainties, is also formulated as a MILP that can be solved to global optimality. We recognize that solving the stochastic version of the problem requires a considerably larger number of binary variables compared to its deterministic counterpart ($3\times(|\mathcal{K}|\times|\mathcal{N}|\times|S|)$ more binary variables). This results in exploring a larger solution space and creating larger rooted trees when utilizing Branch-and-Cut to solve the problem. As a result, addressing the stochastic version is computationally more complex than addressing the deterministic one.

5. Numerical experiments

5.1. Numerical experiments description

In the following we test the application of our model by means of two distinct cases. The first case utilizes a simplified network based on synthetic data from Athens, Greece. Subsequently, a practical case study is presented with real-world data from the Athens bus network, demonstrating the model's effectiveness for a real transportation system. This study is particularly relevant as the public transport authority of Athens has received a fleet of 140 electric buses in 2024, and is in need of establishing its charging station network. The primary objective of this research is to determine the optimal locations for charging stations and the most suitable types of chargers for the electric buses that will require charging during their operational day.

Across all model applications, several key considerations remain consistent. The main focus is the greater Athens metropolitan area, served by 280 bus lines. A subset of these bus lines, on which a total of $\mathcal{K}$ electric buses operate, is selected for the electrification. These bus lines primarily function between start and end stops within Athens Municipality and neighboring municipalities of its central administrative region, since the electric bus fleet will be confined to these areas. Each candidate charging station physical location $v \in \mathcal{V}$ can host multiple chargers – both slow (set $\mathcal{N}_1$) and fast (set $\mathcal{N}_2$) – with the number and type of chargers varying by analysis. Thus, our mathematical model flexibly accommodates different charger configurations to meet diverse charging needs.

In addition to spatial and charging-related parameters, the mathematical model incorporates temporal and electricity-related inputs. Charging can occur at any time throughout the operational day, with all charging processes completed by midnight ($c_l = 12$ a.m.). This continuous time frame is not divided into discrete time slots; instead, charging can take place at any point during the day. Slow chargers operate at $r_1 = 30$ kWh/h and fast chargers at $r_2 = 120$ kWh/h. According to the specifications of the bus manufacturer (Abel, 2024), each bus $k \in \mathcal{K}$ has a minimum and maximum state of charge ($SOC_k^{\min} = 20$ kWh, $SOC_k^{\max} = 100$ kWh). The sufficient level of charge SOC_k^{suf} that each bus k can reach after completing the charging process is defined as a percentage ω_k of $SOC_k^{\max}$. In more detail, $\omega_k = 65\%$ if charging occurs before 6 p.m., 50% from 6 p.m. to 9 p.m., and 35% from 9 p.m. to midnight. The decreasing percentage threshold towards the end of the day reflects an effort by the charging system to provide electric buses with sufficient energy to complete their final scheduled trips. It is assumed that all buses fully charge after midnight before the next operational day.

For the successful assignment of electric buses to the charging stations with respect to their arrival time and the overall trip schedules, several additional temporal parameters have to be taken into account. These parameters follow consistent rules across all model instances. Starting with the completion time parameter τ_k, we have predefined these times to approximate the bus timetables of the respective lines, ensuring that the charging needs of electric buses $k \in \mathcal{K}$ occur throughout the entire day. An average speed of 26 km/h was deemed most suitable for the case study examined in this paper based on velocity statistics from the Athens Urban Transportation Organization (OASA).

In the deterministic approach, each electric bus was considered to consume an average of $e = 0.84$ kWh/km en route to the charging station, as specified by the electric bus manufacturer (Abel, 2024). This model of electric buses has been in operation in the Athens transportation network since May 2024. The state of charge (SOC_k) of each bus $k \in \mathcal{K}$ upon completion at the final stop was determined based on the series of trips assigned to each electric bus. Following consultations with the Athens Transportation Organization and based on their experience with integrating electric buses into Athens' bus fleet, a weight of $\gamma = 1.5$ was deemed appropriate for the total deadheading time in the main objective function.

All the cases are represented using the mathematical model detailed in Sections 3 and 4. The model was programmed in Python 3.12 and was solved using a Branch-and-Cut algorithm implemented by the commercial solver Gurobi 12.0.1. The experiments were conducted on a conventional computer machine with a 2.3 GHz processor and 32 GB of RAM.

5.2. Inter-station travel time and energy consumption scenarios

During the course of a day, electric buses may experience fluctuations in their inter-station travel times and the duration required to reach their designated charging locations, causing these times to significantly vary from day to day. These fluctuations can also be observed in the energy consumption of electric buses en route to the assigned charging location, potentially leading to rapid battery depletion and reduced energy efficiency. In the following, the methodology used to generate scenarios reflecting these time and energy-related uncertainties within our model cases is described. For the scenario generation, it is essential to sample the aforementioned uncertain inter-station travel time and energy parameters from a predefined distribution. Selecting the appropriate distribution type is a critical step in our sampling methodology, as the outputs should closely represent real-time bus travel and battery energy consumption conditions.

In past studies (El Faouzi and Maurin, 2007; Mazloumi et al., 2010; Wu et al., 2015; Qi et al., 2018; Rahman et al., 2018), electric bus travel times and battery energy consumption during their trips were best represented using either a normal or a log-normal distribution, contingent upon the characteristics of the data and the nature of variability. While both distribution types are suitable for modeling time and energy segments of an electric bus, the log-normal distribution is typically more appropriate for representing *travel times* and *energy consumption* due to its inherent ability to positively restrict values and its better fit to reflect the skewed nature of the data (Wang et al., 2012; Liu and Liang, 2021). Therefore, a log-normal probability distribution is used to sample the deadheading travel times ($t_{s,kj}$) and battery energy consumption (e_s) of electric buses traveling to charging stations. In contrast, for the completion time ($\tau_{s,k}$) of each bus $k \in \mathcal{K}$, a normal probability distribution is selected (Singh et al., 2024).

For the energy consumption distribution, the energy consumed by an electric bus was sampled within the range of $e^{\min} = 0.65$ kWh/km and $e^{\max} = 1.20$ kWh/km. For both the toy network and the Athens case study, each uncertain parameter – $\tau_{s,k}$, $t_{s,kj}$, and e_s – was sampled across $|S| = 1000$ scenarios. Each model case with $|S|$ scenarios was executed five times using different $\beta(\%)$ values – $\beta = 100\%, \beta = 95\%, \beta = 80\%, \beta = 75\%, \beta = 60\%$ – to assess the impact of varying level of strictness in satisfying all the constraints under worst-case scenarios. All $\beta(\%)$ values, except for $\beta = 100\%$, represent the implementation of chance constraints in (53), (56), and (59), requiring the expressions $C_{s,kj} \geq 0$, $C_{1,s,kj} \geq 0$, and $C_{2,s,kj} \geq 0$ to hold in at least $\beta(\%)$ of the $|S|$ scenarios. In contrast, $\beta = 100\%$ represents the implementation of stochastic constraints in (53), (56), and (59), enforcing the conditions $C_{s,kj} \geq 0$, $C_{1,s,kj} \geq 0$, and $C_{2,s,kj} \geq 0$ to be satisfied across all $|S|$ scenarios.

5.3. Demonstration of the toy network

5.3.1. Deterministic approach

To ensure the reproducibility of our model, we begin our experimentation by demonstrating its application for a small-scale scenario using synthetic data from the central area of Athens — see Fig. 1. In this study area, we consider four candidate charging station locations ($|\mathcal{V}| = 4$), two of which can accommodate up to one slow charger each ($\lambda_{1v} = 1$), and the remaining two locations up to one fast charger each ($\lambda_{2v} = 1$). Specifically, candidate chargers #1 and #2 are slow (set $\mathcal{N}_1$), and candidate chargers #3 and #4 are fast (set $\mathcal{N}_2$). Thus, subset $\mathcal{N}_1$ includes {1, 2} and subset $\mathcal{N}_2$ includes {3, 4}.

In Fig. 1, the final stops of each electric bus $k \in \mathcal{K}$ that require charging are marked with brown color. In this small-scale (toy) network, we consider eleven bus lines operated by electric buses, each with one electric bus that requires charging during the day ($|\mathcal{K}| = 11$). The assignment of one electric bus requiring charging per line each day is based on the preliminary planning by the public transport authority, necessitating only one charging detour from the original schedule during operating hours. However, more electric buses per line can be accommodated without loss of generality. All eleven buses need charging after the completion of their shifts at their final stops.

Before proceeding to the model solution and the determination of the optimal installation sites for slow and fast chargers, it is necessary to mention the state of charge of each electric bus k at the final stop (SOC_k), presented in Table 3, as well as the deadheading time between the final stop and the potential charger j (t_{kj}), presented in Table 4. Additionally, the synthetically

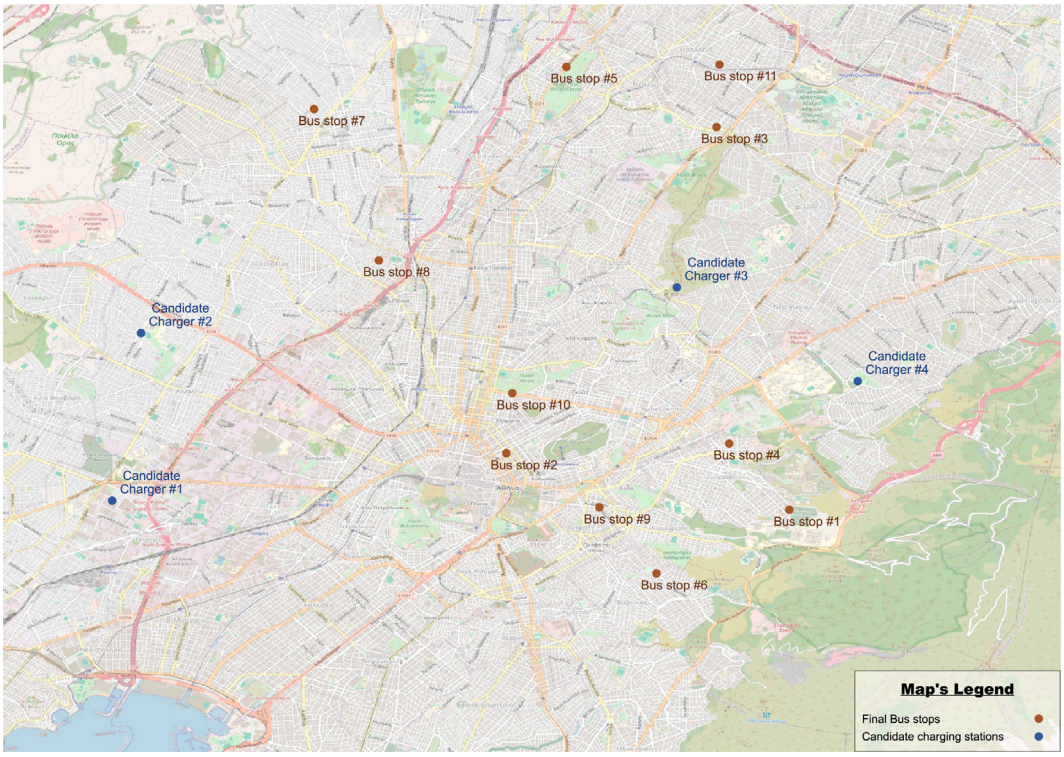

Fig. 1. Toy bus network example. The final stops of the eleven electric buses are shown in brown, while the potential charging station physical locations are indicated in blue.

Table 3
State of Charge of each electric bus $k \in \mathcal{K}$ (SOC_k) at the last stop (kWh).

k	1	2	3	4	5	6	7	8	9	10	11
SOC_k	25	29	42	26	42	40	34	32	26	41	47

Table 4
Estimated deadheading time t_{kj} (in minutes) between the final stop of each electric bus $k \in \mathcal{K}$ and the potential charging station $j \in \mathcal{N}$.

Line $k \in \mathcal{K}$	Charging station option $j \in \mathcal{N}$			
	1	2	3	4
1	22.80	23.10	10.22	5.96
2	13.42	13.32	9.12	12.22
3	25.85	21.27	6.98	11.85
4	20.91	20.35	6.90	5.08
5	24.02	18.28	10.12	16.62
6	18.59	20.16	12.23	10.65
7	18.06	11.20	14.39	21.68
8	13.63	8.58	10.10	16.92
9	16.41	17.13	9.75	10.23
10	14.23	12.76	7.15	11.64
11	27.66	22.59	9.63	14.30

generated temporal attributes of the toy network, which is the completion time when a bus k arrives at its final stop and requires charging (τ_k), are presented in Table 5.

Solving our MILP model with Branch-and-Cut, its optimal solution recommends the installation of charger #2 (slow charger), as well as chargers #3 and #4 (fast chargers) from the pool of $\mathcal{N}$ options. This solution results in a total deadheading time of 94.70 min and zero queue waiting time for all eleven electric buses $\mathcal{K}$. Table 6 presents the optimal assignment of buses $k \in \mathcal{K}$ to chargers $j \in \mathcal{N}$ (q_{kj}) and the charging start (f_{kj}) and end times (l_{kj}) of each bus k to the assigned charging location j. Table 6 also shows the arrival time of each bus k to the assigned charger j, which is the total of the completion time and the deadheading

Table 5
Completion time τ_k of each electric bus $k \in \mathcal{K}$ at the last stop requiring charging (in minutes past midnight).

k	1	2	3	4	5	6	7	8	9	10	11
τ_k	799.4	734.7	886.1	866.5	977.8	902.2	875.5	1027.9	1008.3	1020.6	1173

Table 6
Assignment of electric buses $k \in \mathcal{K}$ to chargers $j \in \mathcal{N}$ and the arrival ($\tau_k + t_{kj}$), charging start (f_{kj}) and end (l_{kj}) time values of each bus k at the assigned charging location j (in minutes past midnight).

q_{kj}	$\tau_k + t_{kj}$	f_{kj}	l_{kj}
(1,4)	805.36	805.36	826.44
(2,3)	743.82	743.82	763.48
(3,3)	893.08	893.08	905.85
(4,4)	871.58	871.58	892.01
(5,3)	987.92	987.92	1001.26
(6,4)	912.85	912.85	927.29
(7,2)	886.70	886.70	956.86
(8,2)	1036.48	1036.48	1108.73
(9,4)	1018.53	1018.53	1039.89
(10,3)	1027.75	1027.75	1041.05
(11,3)	1182.63	1182.63	1185.88
Objective Function Value: 142.05			

duration ($\tau_k + t_{kj}$). This illustrates that upon arrival at the charging location, charging begins immediately. Consequently, the total queue waiting time, calculated as the subtraction of ($\tau_k + t_{kj}$) from f_{kj}, is zero for all electric buses.

Given the optimal solution and the corresponding allocation of each electric bus $k \in \mathcal{K}$ to the charging location options $j \in \mathcal{N}$, it is evident that, at the toy network implementation, model's assignment aligns well with expectations: all electric buses are assigned to their nearest charging location – with one exception – and all buses charge immediately upon arrival at the respective charging site without any waiting time. The exception is bus line #9, which is not assigned to its nearest fast charging station #3, as indicated by its corresponding t_{kj} values – see Table 4 – and instead, it is assigned to its second nearest, the fast charger #4. This deviation can be explained by the fact that if electric bus #9 had been assigned to its nearest charging option #3, it would have caused a delay in the charging start time of bus #10, which is also assigned to charger #3 – as can be seen in Table 6. Consequently, bus #10 would incur a non-zero queue waiting time. By assigning bus #9 to the second nearest charging location #4, this waiting time is avoided.

The initial demonstration showcases that our model does not assign two electric buses to the same charger simultaneously, and achieves its twofold objective: minimization of the overall deadheading costs and reduction of queue waiting times from the arrival of each bus k at the charger j until the beginning of its charging process.

5.3.2. Modeling uncertainties with stochastic and chance constraint approaches

To incorporate time and energy-related uncertainties into the toy network, we first generate 1000 scenarios ($|S|$) for the bus completion times ($\tau_{s,k}$), deadheading duration ($t_{s,kj}$), and energy consumption per traveled distance (e_s) for each electric bus-charging location combination (k, j). After introducing these 1000 different values of τ_k, t_{kj}, and e parameters into our mathematical problem, we apply variations in the $\beta(\%)$ parameter to constraints (53), (56), and (59), as well as constraints (42), (44)–(45), (47), (49)–(52), (54)–(55), (57)–(58), (61)–(62), and the objective function (60).

All scenarios $s \in S$ with each $\beta(\%)$ modification share the same normal distribution sampling of $\tau_{s,k}$ and log-normal distribution of e_s parameters — refer to Figs. 2 and 3. For clarity issues, the log-normal distribution sampling of the $t_{s,kj}$ parameter is depicted only for combinations of buses $k \in \mathcal{K}$ and charging locations $j \in \mathcal{N}$ that are actually assigned to each other ($q_{kj} = 1$) — refer to Fig. 4. Across all $\beta(\%)$ modifications, the optimal solution, derived by Gurobi's Branch-and-Cut algorithm, remained consistent in terms of the charging station installation locations and the assignment of each bus k to charger j, matching the results from the deterministic approach of the toy network.

At the toy network level, the key differences between the outcomes of the deterministic and the stochastic-chance constrained approaches lie in the charging start f_{kj} and end times l_{kj} of each electric bus $k \in \mathcal{K}$ to the assigned charging station $j \in \mathcal{N}$, as shown in Table 7. It is important to note that all buses k, assigned to the same charger j, are scheduled sequentially based on their arrival times ($\tau_k + t_{kj}$), ensuring that their charging processes do not overlap. The queue waiting times for all chance-constrained approaches, including the stochastic one ($\beta = 100\%$), are all zero, similar to the corresponding deterministic case. None of the f_{kj} and subsequently the l_{kj} values of each bus k to the assigned charger j approximate the corresponding deterministic values, except for the ones in the most-relaxed chance-constrained approach with $\beta = 60\%$. In particular, under the stochastic approach and in scenarios with chance constraints nearing to $\beta = 100\%$, all electric buses tend to start their charging process (f_{kj}) significantly later in their operation day compared to the deterministic method. This delay is generally anticipated due to the requirement of constraints (53), (56), and (59) to hold true for the vast majority of the 1000 scenarios.

Overall, the start time of charging of each trip $k \in \mathcal{K}$ to the assigned charging location $j \in \mathcal{N}$ (f_{kj}) across all $\beta(\%)$ variations (Table 7) is precisely equal to the maximum total of the completion and deadheading time ($\tau_k + t_{kj}$) of the respective combination of

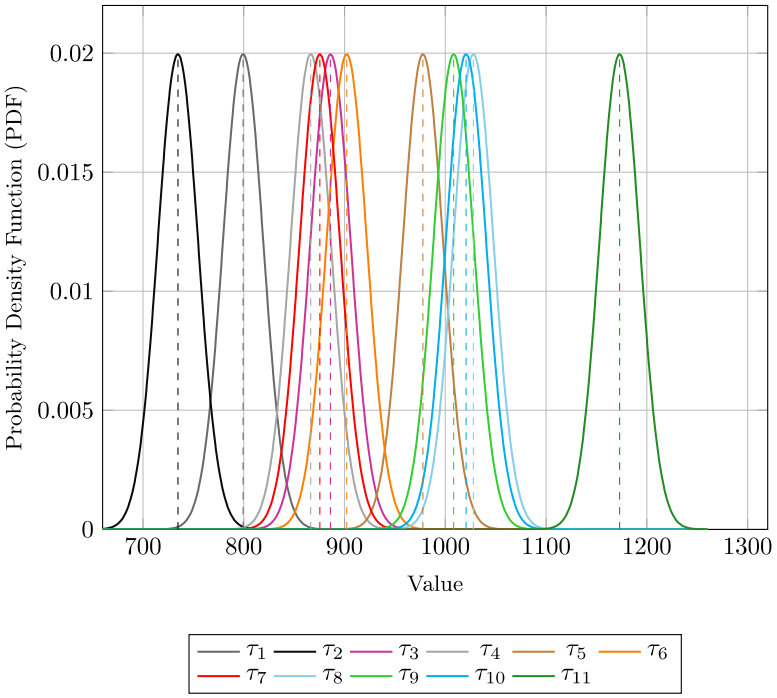

Fig. 2. Completion time τ_k (in minutes past midnight) of each electric bus $k \in \mathcal{K}$ at the last stop requiring charging across all scenarios $s \in S$ – Normal distribution in the toy network.

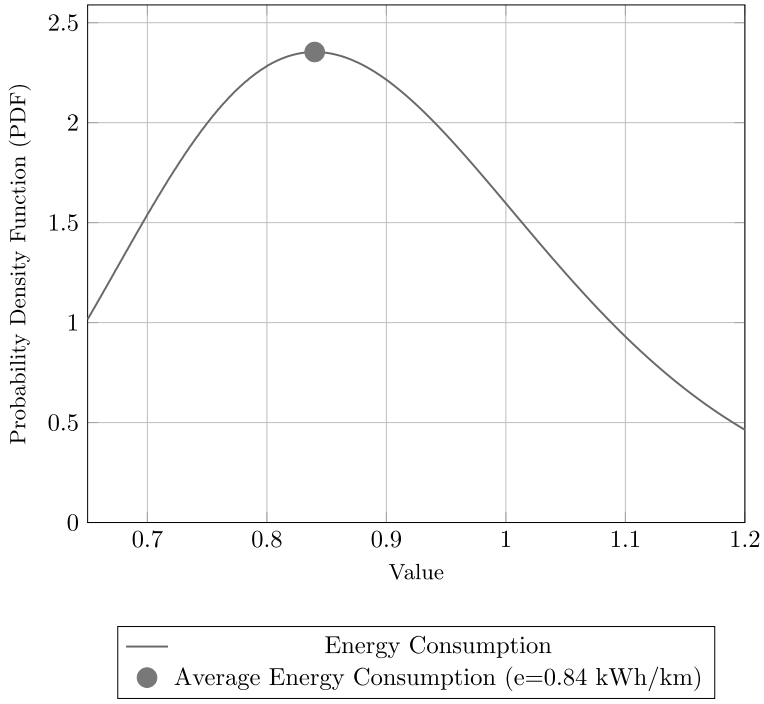

Fig. 3. Battery energy consumption per traveled distance e (in kWh/km) between the final stop of each electric bus $k \in \mathcal{K}$ and its assigned charging location $j \in \mathcal{N}$ across all scenarios $s \in S$ – Log-normal distribution in the toy network.

bus k and charger j across the scenarios $|S|$, which is typically their arrival time. As the β percentage value decreases towards 60%, relaxing the constraints (53), (56), and (59), the objective function value also decreases — see Table 7. Regarding the energy-related

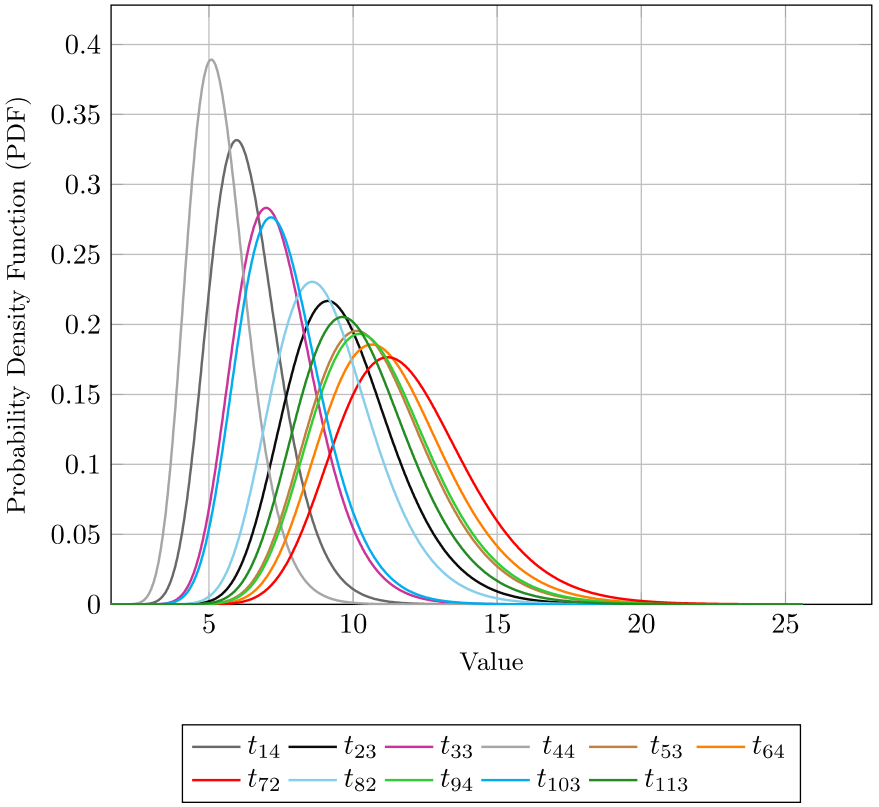

Fig. 4. Estimated deadheading time t_{kj} (in minutes) between the final stop of each electric bus $k \in \mathcal{K}$ and its assigned charging station location $j \in \mathcal{N}$ across all scenarios $s \in S$ – Log-normal distribution in the toy network.

Table 7
Charging start (f_{kj}) and end (l_{kj}) time values of each electric bus $k \in \mathcal{K}$ at the assigned charging location $j \in \mathcal{N}$ across all β (%) variations (in minutes past midnight).

q_{kj}	β % percentage variations									
	100 (%)		95 (%)		80 (%)		75 (%)		60 (%)	
	f_{kj}	l_{kj}	f_{kj}	l_{kj}	f_{kj}	l_{kj}	f_{kj}	l_{kj}	f_{kj}	l_{kj}
(1,4)	870.65	892.19	838.93	860.48	821.87	843.22	818.95	840.28	810.47	831.69
(2,3)	808.03	828.40	778.58	798.95	762.23	782.29	758.84	778.82	750.40	770.23
(3,3)	956.59	969.90	926.40	939.71	911.23	924.32	907.85	920.87	898.77	911.67
(4,4)	936.58	957.41	904.98	925.80	888.83	909.48	885.50	906.32	876.47	897.19
(5,3)	1053.59	1067.72	1020.99	1035.12	1007.54	1021.33	1004.25	1017.95	994.69	1008.22
(6,4)	974.51	986.20	946.23	961.49	930.98	945.93	927.81	942.63	919.15	933.78
(7,2)	959.01	1032.66	918.58	992.23	902.99	975.14	900.23	971.97	891.99	962.98
(8,2)	1103.84	1148.76	1069.72	1144.64	1053.53	1127.30	1050.77	1124.23	1042.78	1115.67
(9,4)	1091.47	1106.13	1052.91	1075.07	1036.43	1058.56	1032.32	1054.04	1024.33	1045.92
(10,3)	1097.26	1103.62	1062.44	1076.30	1045.02	1058.87	1041.48	1055.03	1033.31	1046.75
(11,3)	1249.59	1253.59	1218.06	1222.06	1200.29	1203.97	1197.13	1200.72	1188.79	1192.22
Objective Function Value:	**872.76**		**517.57**		**360.73**		**332.99**		**269.41**	
Total Queue Waiting Time (min):	**0**		**0**		**0**		**0**		**0**	

uncertainty part of all electric buses, Table 8 presents the remaining battery levels upon arrival at the assigned charging locations j across all $\beta(\%)$ variations. Even in the most stringent stochastic approach, where energy consumption reaches the upper limit of $e = 1.2$ kWh/km to ensure that constraints (59) are always satisfied, all battery levels remain above the $SOC_k^{\min}$ threshold across all scenarios $|S|$. Finally, the charging completion time of each bus k (l_{kj}) adheres to the designated time horizon, from the start of the operational day until $c_l = 12$ a.m., as set in all experiments. This adherence is maintained despite the challenges introduced by the scenario generation within the model.

Table 8
Remaining State of Charge of each electric bus $k \in \mathcal{K}$ upon their arrival at the charging location $j \in \mathcal{N}$ across all β (%) variations (kWh).

k	β % percentage variations				
	100 (%)	95 (%)	80 (%)	75 (%)	60 (%)
1	21.90	21.90	22.30	22.34	22.58
2	24.26	24.26	24.87	25.03	25.34
3	38.37	38.37	38.84	38.96	39.20
4	23.36	23.36	23.70	23.36	23.55
5	36.73	36.73	37.41	37.60	37.93
6	34.46	34.46	35.11	35.37	35.72
7	28.17	28.17	28.93	29.13	29.50
8	27.54	27.54	28.11	28.27	28.55
9	20.68	20.68	20.72	21.55	21.82
10	37.28	37.28	37.30	37.89	38.13
11	41.99	41.99	42.64	42.81	43.13

Table 9
Allocation of slow (set $\mathcal{N}_1$) and fast (set $\mathcal{N}_2$) charging types to the candidate charging station physical locations (set $\mathcal{V}$).

$\mathcal{V}$	$\mathcal{N}_1$	$\mathcal{N}_2$
1	1,3	2
2	5	4,6
3	7	8
4	9	10
5	11	12
6	13	14
7	15	16
8	17	18
9	19	20

5.4. Case study on the bus network of central Athens

5.4.1. Deterministic approach

In this real-world model application, we employed actual data from the central area of Athens. The experiments outlined below consider both deterministic and stochastic chance-constrained approaches. When a site is selected by the model, it may host either or both types of chargers. Consequently, set $\mathcal{V}$ is comprised of nine locations ($|\mathcal{V}| = 9$) and set $\mathcal{N}$ of twenty candidate charging options ($|\mathcal{N}| = 20$): ten slow chargers and ten fast chargers. Specifically, charging options #1, #3, #5, #7, #9, #11, #13, #15, #17, and #19 represent slow chargers (set $\mathcal{N}_1$), while options #2, #4, #6, #8, #10, #12, #14, #16, #18, and #20 correspond to fast chargers (set $\mathcal{N}_2$). Thus, $\mathcal{N}_1 = \{1, 3, 5, 7, 9, 11, 13, 15, 17, 19\}$ and $\mathcal{N}_2 = \{2, 4, 6, 8, 10, 12, 14, 16, 18, 20\}$. The nine sites (set $\mathcal{V}$) proposed for charger installations align with the actual bus depots in the Attica region, as Athens' public transport authority plans to install electric bus charging infrastructure at some of these locations. It is acknowledged that some bus depots are located far from the borders of the municipality of Athens; however, it was deemed appropriate for our model's candidate charging locations to include all potential options. Each candidate location can typically host up to two charging options (one slow, $\lambda_{1v} = 1$, and one fast charger, $\lambda_{2v} = 1$), except for locations #1 and #2, which can accommodate up to three charging options. Specifically, location #1 can host up to one fast charger ($\lambda_{2v} = 1$) and two slow chargers ($\lambda_{1v} = 2$), while location #2 can host up to one slow charger ($\lambda_{1v} = 1$) and two fast chargers ($\lambda_{2v} = 2$). Table 9 summarizes the allocation of the offered charging types to the physical locations of charging stations.

For the electric bus network, we have selected 10 distinct bus lines, each serviced by three electric buses, resulting in a total of 30 electric buses ($|\mathcal{K}| = 30$). These lines were chosen from Athens' extensive network of 280 bus routes based on the geographical locations of their terminal stops, ensuring that they are situated within the boundaries of the Athens Municipality. In compliance with the Athens Urban Transport Organization (OASA) as of July 2024, some electric buses have shown no need for charging at the end of their operational day. To align with this data, the frequency of the charging requirements for each bus throughout the day has been determined accordingly, with each bus requiring a single charging session per operational day. Fig. 5 presents the detailed layout of the bus network utilized in this case study.

The state of charge for each of the thirty electric buses $k \in \mathcal{K}$ at their final stops (SOC_k) has been set as shown in Table 10, as well as the travel distance between the terminal stop of each bus k and the candidate charging station $j \in \mathcal{N}$ (t_{kj}) are presented in a 30 × 20 Table A.17 in the Appendix. Additionally, the completion times of each bus k at their final stops requiring charging (τ_k) are shown in Table 11.

Based on these data, the model's optimal solution (Table 12) indicates that chargers should be installed at two physical locations $\mathcal{V} = \{1, 8\}$ out of the nine available with five charging types — three slow chargers $\mathcal{N}_1 = \{1, 3, 17\}$ and two fast chargers $\mathcal{N}_2 = \{2, 18\}$– distributed among these two locations. This solution was computed using Gurobi's Branch-and-Cut solution method, similar to the approach used in the toy network, resulting in an optimal total deadheading time of 156.25 min and a zero total queue waiting time

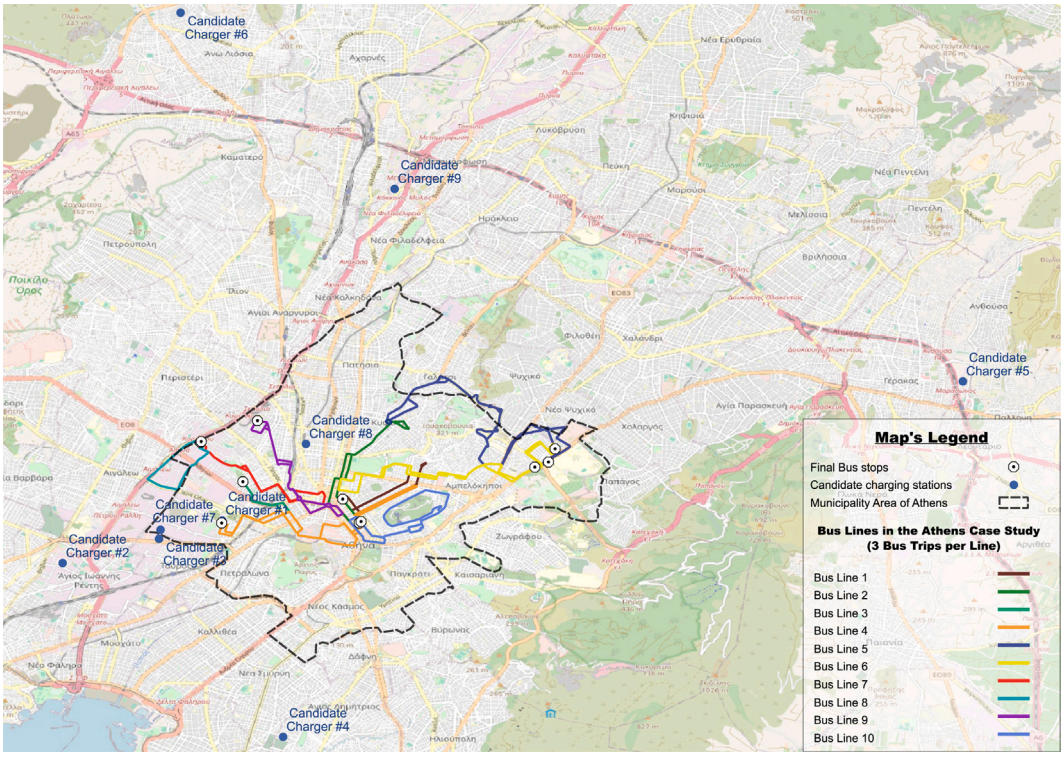

Fig. 5. Athens network of the electric bus lines, along with the proposed charging station physical locations.

Table 10
State of Charge of each electric bus $k \in \mathcal{K}$ (SOC_k) at the last stop (kWh).

k	1	2	3	4	5	6	7	8	9	10
SOC_k	32	33	28	30	28	35	28	32	29	25
k	11	12	13	14	15	16	17	18	19	20
SOC_k	31	33	35	26	27	35	29	26	30	33
k	21	22	23	24	25	26	27	28	29	30
SOC_k	31	33	35	28	29	29	34	32	33	31

Table 11
Completion time τ_k of each electric bus $k \in \mathcal{K}$ at the last stop requiring charging (in minutes past midnight).

k	1	2	3	4	5	6	7	8	9	10
τ_k	712.3	736.7	795	848.3	862.7	680	871.3	820.7	788	917.3
k	11	12	13	14	15	16	17	18	19	20
τ_k	804.7	911	799.3	867.7	807	818.3	832.7	1006	991.3	868.7
k	21	22	23	24	25	26	27	28	29	30
τ_k	977	1068.3	961.7	1028	1118.3	953.7	1095	1029.3	1181.7	1112

for all thirty buses across the ten examined distinct lines. Table 12 displays the charging start (f_{kj}) and charging end times (l_{kj}) of each electric bus $k \in \mathcal{K}$ at the assigned charging location $j \in \mathcal{N}$, along with the total of their completion time and deadheading time ($\tau_k + t_{kj}$). From these totals, it is evident that the charging process for each bus k begins immediately upon arrival at the assigned charging location j. For a more comprehensive presentation of the solution, Table 13 presents the active service time, idle time due to deadheading and charging, and downtime of each bus k, with bus #14 showing the highest downtime. Additionally, buses assigned to slow charging types exhibit significant downtime values.

Given the optimal solution, two charging station locations are selected out of the nine available. Notably, approximately 53% of the electric buses are assigned to charging location #8, while the remaining buses – approximately 47% – are assigned to charging location #1. From a cost-efficiency perspective, the objective of minimizing installation costs is practically achieved, as all thirty buses are assigned to only two charging sites. Additionally, out of the thirty buses, only two are not assigned to their nearest charging location. Instead, these trips are assigned to the second closest charging site, which can be explained by the dual model's objective of minimizing both deadheading time and queue waiting time. It is also noteworthy that the sequence in the charging process for buses assigned to the same charger is successfully achieved.

Table 12
Assignment of electric buses $k \in \mathcal{K}$ (3 electric buses per bus line) to chargers $j \in \mathcal{N}$ and the arrival ($\tau_k + t_{kj}$), charging start (f_{kj}) and end (l_{kj}) time values of each electric bus k at the assigned charging location j (in minutes past midnight).

Lines	q_{kj}	$\tau_k + t_{kj}$	f_{kj}	l_{kj}
#1	(1,18)	715.81	715.81	732.94
	(2,18)	740.21	740.21	756.84
	(3,18)	798.51	798.51	817.64
#2	(4,2)	854.55	854.55	873.19
	(5,18)	867.82	867.82	887.25
	(6,18)	685.12	685.12	711.55
#3	(7,2)	873.76	873.76	892.71
	(8,1)	823.16	823.16	890.95
	(9,3)	790.46	790.46	864.25
#4	(10,2)	917.55	917.55	937.60
	(11,2)	804.95	804.95	822
	(12,1)	911.25	911.25	975.44
#5	(13,17)	810.29	810.29	878.28
	(14,17)	878.69	878.69	964.68
	(15,18)	817.99	817.99	838.98
#6	(16,2)	834.02	834.02	851.88
	(17,18)	843.98	843.95	864.03
	(18,17)	1017.28	1017.28	1103.49
#7	(19,2)	995.74	995.74	1014.05
	(20,3)	873.14	873.14	940.37
	(21,3)	981.44	981.44	1052.67
#8	(22,2)	1072.80	1072.80	1089.62
	(23,2)	966.20	966.20	982.02
	(24,1)	1032.50	1032.50	1109.77
#9	(25,17)	1120.86	1120.86	1164.73
	(26,18)	956.26	956.26	974.73
	(27,18)	1097.56	1097.56	1106.03
#10	(28,18)	1034.42	1034.42	1051.85
	(29,17)	1186.82	1186.82	1224.55
	(30,18)	1117.12	1117.12	1127.55
Objective Function Value: 234.38				
Total Queue Waiting Time (min): 0				
Computation Time (min): 3.62				

Overall, this case study on the Athens city network demonstrated that the model successfully assigned 30 electric buses $k \in \mathcal{K}$ to 20 potential charging options $j \in \mathcal{N}$ across the nine candidate physical locations, requiring to use only two of them.

5.4.2. Modeling uncertainties with stochastic and chance constraint approaches

To incorporate time and energy-related uncertainties into the Athens bus network case study, we follow the same procedure as in the toy network. We first generate scenarios ($|S|$) for the electric bus completion times ($\tau_{s,k}$), deadheading times ($t_{s,kj}$), and energy consumption per traveled distance (e_s) for each combination of buses $k \in \mathcal{K}$ and chargers $j \in \mathcal{N}$. Then, we apply the $\beta(\%)$ variations to the constraints (53), (56), and (59). All scenarios within each β percentage modification share the same normal distribution sampling for the $\tau_{s,k}$ parameter and the same log-normal distribution for the e_s parameter.

Tables 14 and 15 present the optimal locations and types of chargers for charging station installations and the assignment of each bus $k \in \mathcal{K}$ to charger $j \in \mathcal{N}$ (q_{kj}) across all $\beta(\%)$ variations. Evidently, these solutions differ from each other. A commonality among the deterministic, stochastic, and chance-constrained approaches, as observed in Table 14, is that most solutions recommend installing chargers at two specific physical locations $\mathcal{V} = \{1, 8\}$ out of the nine available. Complementary to charging locations #1 and #8, the stochastic approach and several chance-constrained approaches suggest installing chargers at $\mathcal{V} = \{3, 7\}$. Table 14 also shows that both the stochastic approach and the chance constrained approach with $\beta = 75\%$ recommend installing a total of eight chargers, while the chance-constrained approach with $\beta = 95\%$ a total of six chargers. It is also worth mentioning that the chance-constrained approaches with $\beta = 60\%$ and $\beta = 80\%$ recommend the same five chargers at the same locations as the deterministic approach.

The assignment of each bus $k \in \mathcal{K}$ to charger $j \in \mathcal{N}$, which is presented in Table 15, varies significantly across these approaches. In the deterministic approach and the chance-constrained approaches with $\beta = 60\%$ and $\beta = 80\%$, all buses k are assigned to the charging station physical locations $\mathcal{V} = \{1, 8\}$. For the remaining chance-constrained approaches, the percentage of buses allocated to stations #1 and #8 is as follows: 90% in the stochastic approach, $\simeq 93\%$ in the chance-constrained approach with $\beta = 95\%$, and

Table 13
Active service time, idle time due to deadheading and charging, and downtime (%) for each electric bus $k \in \mathcal{K}$ (3 electric buses per bus line) (in minutes) – Athens case study network.

Lines	Electric Buses	Active service time	Idle time due to deadheading	Idle time due to charging	Bus downtime (%)
#1	**1**	402.30	8.51	17.14	5.99%
	2	406.70	8.51	16.64	5.82%
	3	445	8.51	19.14	5.85%
#2	**4**	498.30	6.25	18.64	4.76%
	5	497.70	5.12	19.43	4.70%
	6	350	5.12	15.93	5.67%
#3	**7**	656.30	7.46	18.95	3.87%
	8	455.70	7.46	67.79	14.17%
	9	458	7.46	73.79	15.07%
#4	**10**	537.30	5.25	20.05	4.50%
	11	489.70	5.25	17.05	4.35%
	12	566	5.25	64.18	10.93%
#5	**13**	434.30	10.99	68.00	15.39%
	14	412.70	10.99	86.00	19.03%
	15	397	10.99	21.00	7.46%
#6	**16**	478.30	15.72	17.86	6.56%
	17	462.70	11.28	20.05	6.34%
	18	611	11.28	86.21	13.76%
#7	**19**	661.30	5.44	18.31	3.47%
	20	568.70	5.44	67.23	11.33%
	21	662	5.44	71.23	10.38%
#8	**22**	633.30	6.50	16.82	3.55%
	23	556.70	6.50	15.82	3.85%
	24	608	6.50	77.27	12.11%
#9	**25**	743.30	8.56	43.87	6.59%
	26	638.70	8.56	18.47	4.06%
	27	750	8.56	8.47	2.22%
#10	**28**	669.30	5.12	17.43	3.26%
	29	761.70	5.12	37.73	5.33%
	30	722	5.12	10.43	2.11%

Table 14
Optimal charging station physical locations ($\mathcal{V}$), and charging types ($\mathcal{N} = \mathcal{N}_1 \cup \mathcal{N}_2$) across all $\beta(\%)$ variation approaches.

	$\beta(\%)$ percentage variations														
	100 (%)			95 (%)			80 (%)			75 (%)			60 (%)		
	$\mathcal{V}$	$\mathcal{N}_1$	$\mathcal{N}_2$	$\mathcal{V}$	$\mathcal{N}_1$	$\mathcal{N}_2$	$\mathcal{V}$	$\mathcal{N}_1$	$\mathcal{N}_2$	$\mathcal{V}$	$\mathcal{N}_1$	$\mathcal{N}_2$	$\mathcal{V}$	$\mathcal{N}_1$	$\mathcal{N}_2$
	1	1,3	2	1	1,3	2	1	1,3	2	1	1,3	2	1	1,3	2
	3	7	8	7		16	8	17	18	3		8	8	17	18
	7		16	8	17	18				7	15	16			
	8	17	18							8	17	18			
Total number:	**4**	$N_1 + N_2 = 8$		**3**	$N_1 + N_2 = 6$		**2**	$N_1 + N_2 = 5$		**4**	$N_1 + N_2 = 8$		**2**	$N_1 + N_2 = 5$	

$\simeq 87\%$ in the chance-constrained approach with $\beta = 75\%$. Despite the cost-inefficiency of installing additional charging sites for a small percentage of bus charging demands, the stochastic and chance-constrained approaches allow this to happen.

All solutions, presented in Tables 14 and 15, determined using Branch-and-Cut, resulted in higher objective function values compared to the deterministic approach, though these values diminish as the chance-constrained $\beta(\%)$ value decreases. Regarding the total queue waiting time for all thirty buses, it is negligible in most approaches, except for the chance-constrained approach with $\beta = 95\%$, where it reaches 23.49 min — see Table 15. However, even in this case, where the total queue waiting time is the highest, the maximum delay an electric bus experiences before commencing its charging process is approximately ten minutes. This duration is considered acceptable given the various uncertainties that are taken into consideration at these case studies.

Table 15 also indicates the number of buses that are not assigned to their nearest charging station, with the minimum of three occurring in the chance-constrained approaches with $\beta = 60\%$ and $\beta = 80\%$, and, as expected, the maximum of eight in the stochastic approach ($\beta = 100\%$). Across all approaches, electric buses that are not assigned to their closest charger $j \in \mathcal{N}$ are instead allocated to the second, third, or fourth nearest one. This can be attributed to the twofold model's objective of minimizing not only the deadheading time (t_{kj}) but also the queue waiting time.

From Table A.18 in the Appendix, under the stochastic approach and chance constraints nearing $\beta = 100\%$, buses tend to start their charging process (f_{kj}) significantly later in their operation day compared to the deterministic method. This delay, as occurred

Table 15
Assignment of electric buses $k \in \mathcal{K}$ (3 electric buses per bus line) to chargers $j \in \mathcal{N}$ across all stochastic approaches with different β (%) variations.

q_{kj}	$\beta(\%)$ percentage variations				
Lines	100 (%)	95 (%)	80 (%)	75 (%)	60 (%)
#1	(1,18) (2,18) (3,18)	(1,18) (2,2) (3,2)	(1,18) (2,18) (3,18)	(1,18) (2,18) (3,18)	(1,18) (2,18) (3,18)
#2	(4,2) (5,3) (6,2)	(4,16) (5,3) (6,18)	(4,18) (5,18) (6,17)	(4,8) (5,18) (6,17)	(4,2) (5,18) (6,18)
#3	(7,7) (8,2) (9,2)	(7,2) (8,2) (9,2)	(7,2) (8,3) (9,2)	(7,2) (8,2) (9,3)	(7,2) (8,3) (9,1)
#4	(10,2) (11,1) (12,1)	(10,2) (11,3) (12,2)	(10,2) (11,1) (12,3)	(10,2) (11,2) (12,3)	(10,3) (11,2) (12,2)
#5	(13,18) (14,18) (15,17)	(13,18) (14,2) (15,18)	(13,2) (14,18) (15,18)	(13,17) (14,17) (15,8)	(13,17) (14,17) (15,18)
#6	(16,2) (17,18) (18,17)	(16,17) (17,18) (18,17)	(16,17) (17,2) (18,18)	(16,18) (17,18) (18,18)	(16,2) (17,18) (18,18)
#7	(19,2) (20,8) (21,1)	(19,1) (20,1) (21,2)	(19,18) (20,1) (21,2)	(19,15) (20,1) (21,2)	(19,2) (20,1) (21,1)
#8	(22,3) (23,18) (24,16)	(22,16) (23,18) (24,3)	(22,2) (23,1) (24,3)	(22,16) (23,1) (24,3)	(22,2) (23,2) (24,2)
#9	(25,17) (26,18) (27,18)	(25,18) (26,18) (27,18)	(25,17) (26,18) (27,18)	(25,18) (26,18) (27,17)	(25,18) (26,18) (27,18)
#10	(28,18) (29,17) (30,18)	(28,18) (29,17) (30,18)	(28,17) (29,17) (30,18)	(28,17) (29,17) (30,2)	(28,17) (29,18) (30,2)
Objective Function Value:	**1754.79**	**1265.07**	**825.04**	**745.61**	**572.08**
Total Queue Waiting Time (min):	**1.60**	**23.49**	**1.06**	**3.78**	**0.77**
Buses assigned to their closest charger (out of 30):	**22**	**23**	**27**	**25**	**27**
Computation Time (min):	**6.68**	**16.99**	**255.98**	**684.38**	**5216.55**

in the toy network, is expected due to the stringent requirement for constraints (53) to be satisfied across the vast majority of the $|S|$ scenarios. As we progress to the chance-constrained approach with $\beta = 60\%$, the f_{kj} values approximate those of the deterministic approach. Based on the f_{kj} values of the Table A.18, the sequence of the charging process of electric buses $k \in \mathcal{K}$ assigned to the same charger $j \in \mathcal{N}$, and the charging completion time (l_{kj}) of all buses within the designated time horizon of $c_l = 12$ a.m. were confirmed. Additionally, in the Appendix, Table A.19 presents the remaining battery levels of all buses k upon arrival at their assigned charging location j across all $\beta(\%)$ variations, while Table A.20 presents the active service times, idle times due to deadheading and charging, and downtimes of buses under the most stringent approach — the stochastic one. From these results, it can be concluded that none of the stochastic approaches violate the energy threshold $SOC_k^{\min}$, and the most elevated downtimes are observed in buses assigned to slow charging types, with the highest downtime occurring in electric bus #15.

Based on the results of the above experiments solved both deterministically and involving time and energy-related uncertainties through the stochastic and chance-constrained approaches, our findings demonstrate that the problem can be effectively addressed with Branch-and-Cut. Computation times for stochastic approaches, which are presented in Table 15, were acceptable for mid-sized networks, except for the chance-constrained approaches with $\beta = 75\%$ and $\beta = 60\%$. It is important to note that solving the MILP with uncertainties (stochastic optimization model) requires significantly more computation time compared to the deterministic optimization model due to:

- The need to incorporate all the sampled travel time and energy consumption scenarios $|S|$ into the optimization process, leading to a higher number of parameters and variables ($3 \times (|\mathcal{K}| \times |\mathcal{N}| \times |S|)$ additional binary variables).
- The requirement for constraints (53), (56), and (59) to hold true for the $\beta(\%)$ variations in such an extensive network, which results in a wide-ranging exploration of the rooted Branch-and-Cut tree to find a globally optimal solution (Huang et al., 2021; Morrison et al., 2016; Gkiotsalitis et al., 2023a).

Table 16
Total deadheading, queue waiting, and excessive times (in minutes) from the simulation of the solutions obtained in Section 5.4.2 across new scenarios $s \in S$.

	β (%) percentage variation simulations				
	100 (%)	95 (%)	80 (%)	75 (%)	60 (%)
Total Deadheading Time (min):	279.12	291.52	276.14	279.74	268.99
Total Queue Waiting Time (min):	22.11	93.30	34.51	8.52	45.03
Total Excessive Time (min):	1858.50	1936.05	1862.13	1835.93	1870.07

5.4.3. Simulation-based performance evaluation of the optimal solutions obtained from the stochastic and chance constraint approaches

Besides the initial sampling of $\tau_{s,k}$, $t_{s,kj}$, and e_s described above, an additional set of samples, independent from the previous one, is drawn for evaluating the performance of the optimal solutions derived by the stochastic and chance constraint optimization approaches. The new samples of $\tau_{s,k}$, $t_{s,kj}$, and e_s, which are used to evaluate the performance of the optimal solutions proposed by the stochastic and chance-constrained models, contain different scenarios ($|S|$) from the initial ones.

We now proceed to the evaluation of the performance of the solutions obtained from the stochastic and chance constraint optimization approaches in Section 5.4.2. To perform this task, for each obtained solution in Tables 14 and 15, we performed simulations using newly sampled electric bus completion times, deadheading times, and battery energy consumption data to test its performance in terms of deadheading and queue waiting times for charging purposes. As one might have expected, the deadheading times and queue waiting times of each solution differ when applied to new scenarios. The results of this simulation-based evaluation of each solution are presented in Table 16.

For each tested solution, Table 16 presents the deadheading time, the total queue waiting time, and the total excessive time (the sum of both), which corresponds to the objective function value of the respective solutions in Table 15. One can notice that the total excessive times in Table 16 approach the objective function of the stochastic approach in Table 15, due to their shared stochastic nature. More specifically, constraints (53), (56), and (59) were enforced to always hold true during the simulations to reflect the real conditions, ensuring all buses $k \in \mathcal{K}$ are charged, and their battery levels remain above $SOC_k^{\min}$. However, differences arise even with the stochastic approach due to the different completion time ($\tau_{s,k}$), deadheading duration ($t_{s,kj}$), and energy consumption per traveled distance (e_s) scenarios generated in the simulation process. These time and energy-related distributions significantly affect the final configuration of charging station types, the assignment of each bus k to potential chargers $j \in \mathcal{N}$ (q_{kj}), and the charging schedules. Higher time and energy values may necessitate additional charging stations or types to meet the charging demand and the model's dual objective, maintain charging sequences, and ensure buses are served within the operational day horizon (in our case, from the start of the operational day until $c_l = 12$ a.m.), without depleting the bus battery levels below the established thresholds. This contrasts with scenarios where more balanced-distributed parameters allow the same charging station locations to successively meet all charging demands within the designated time frame.

Regarding the total queue waiting times, the simulation results yield non-zero values — see Table 16 – which are higher than the corresponding values of the respective solutions in Table 15. Among all tested configurations, the optimal solution derived from the chance-constrained method with $\beta = 75\%$ provides the best results in terms of total excessive time and queue waiting time. As detailed in Table 14, this approach recommends the same set of charging station locations, $V = \{1, 3, 7, 8\}$, with locations #1 and #8 favored by most electric buses, and the same total number of chargers $j \in \mathcal{N}$ (8 in total) as the stochastic solution ($\beta = 100\%$). However, the two solutions differ in both the allocation and types of chargers installed at certain charging sites. Notably, the solution for $\beta = 75\%$ recommends a more uniform distribution of the electric bus charging demands across charging sites, which reduces overlaps in charging schedules and leads to a slight improvement in overall simulation performance compared to the solution for $\beta = 100\%$, as evidenced in Table 16.

In contrast, the simulation of the optimal solution from the chance-constrained method with $\beta = 95\%$ results in the poorest total excessive time and highest total queue waiting time, despite recommending the second most extensive infrastructure configuration — three charging locations and six charging types. Interestingly, even the simulation results of the chance-constrained approaches with $\beta = 60\%$ and $\beta = 80\%$, which recommend only two, yet highly critical, charging locations (#1 and #8), and fewer charging types (five in total), outperform the simulation results of the solution for $\beta = 95\%$ due to a more effective distribution of charging demand at these key locations. Therefore, it can be inferred that, under time and energy-related uncertainties, the diversity of charging types and the balanced distribution of charging demand across charging locations are more influential factors than the number of charging locations themselves, especially at critical charging sites that accommodate a large share of the total demand.

Concluding remarks

We propose a novel mathematical optimization model for the Electric Bus Charging Station Location Problem (EB-CSLP) within a network of electric buses. The model considers multiple charger types and aims to maintain time continuity and sequence between electric buses at any charger type, without predefined charging time slots. The objective is to minimize two time-related factors: (a) the deadheading time, which is the time electric buses travel without passengers between their final stop and the potential charging stations, and (b) the queue waiting time, which is the elapsed time between the arrival of the electric bus at the charger and the start of the charging process.

The model imposes several constraints to maintain the state of charge of each electric bus at acceptable levels and prevent overlapping charging assignments at shared chargers. It also accounts for uncertainties in inter-station travel times, including

completion times, deadheading durations, and energy consumption per traveled distance while electric buses head to the charging sites. To simulate real-world conditions, multiple scenarios were generated to capture the variability of these uncertain parameters, particularly relevant for electric buses equipped with new and untested technologies. The model is tested in two distinct cases: i) a toy network with synthetic data from the transportation network of Athens, Greece, and (ii) a real-world case study in central Athens. Experimental results indicate that the diversity of charging types and a uniform distribution of charging demand across charging locations are more critical under time- and energy-related uncertainties than simply increasing the number of charging sites. Moreover, implementing chance constraints with $\beta = 75\%$, which ensures stochastic constraint satisfaction in at least 75% of all scenarios, yielded the best performance when tested on new scenarios with unseen data.

Taking into account the model's assumptions and limitations, future research could explore the simultaneous charging of multiple vehicles at a single charger. This would involve examining the capacity and constraints of power grids near the charging stations, as infrastructure upgrades and smart energy management systems might be necessary. Additionally, the dynamic routing of electric buses to charging locations could be investigated to account for unforeseen events affecting travel paths. Future studies should also incorporate cost considerations for charging installations, including energy pricing, to provide a more comprehensive comparison of the cost efficiency of the model under both deterministic and stochastic perspectives. Finally, metaheuristic solution approaches can be employed to reduce computational costs when applying our method to large problem instances.

CRediT authorship contribution statement

Androniki Dimitriadou: Writing – original draft, Visualization, Validation, Software, Methodology, Investigation, Formal analysis, Data curation, Conceptualization. **Konstantinos Gkiotsalitis:** Writing – review & editing, Supervision, Methodology, Funding acquisition, Conceptualization. **Tao Liu:** Writing – review & editing, Methodology. **Oded Cats:** Writing – review & editing, Methodology.

Declaration of competing interest

The authors declare that they have no known competing financial interests or personal relationships that could have appeared to influence the work reported in this paper.

Acknowledgments

The present work is partially funded by the metaCCAZE Project (Flexibly adapted MetaInnovations, use cases, collaborative business and governance models to accelerate deployment of smart and shared Zero Emission mobility for passengers and freight). This project has received funding from the European Union's Horizon Europe research and innovation programme under grant agreement No. 101139678.

Appendix

See Tables A.17–A.20.

Table A.17
Estimated deadheading time t_{kj} (in minutes) between the final stop of each electric bus $k \in \mathcal{K}$ (3 electric buses per bus line) and the potential charging station $j \in \mathcal{N}$ – Athens case study network.

Line	Buses	Charging station option $j \in \mathcal{N}$																			
		1	2	3	4	5	6	7	8	9	10	11	12	13	14	15	16	17	18	19	20
#1	**1**	5.66	5.66	5.66	13.38	13.38	13.38	8.41	8.41	13.88	13.88	29.02	29.02	29.28	29.28	8.57	8.57	8.51	8.51	17.76	17.76
	2	5.66	5.66	5.66	13.38	13.38	13.38	8.41	8.41	13.88	13.88	29.02	29.02	29.28	29.28	8.57	8.57	8.51	8.51	17.76	17.76
	3	5.66	5.66	5.66	13.38	13.38	13.38	8.41	8.41	13.88	13.88	29.02	29.02	29.28	29.28	8.57	8.57	8.51	8.51	17.76	17.76
#2	**4**	6.25	6.25	6.25	13.77	13.77	13.77	8.86	8.86	12.65	12.65	28.66	28.66	30.86	30.86	9.11	9.11	5.12	5.12	19.10	19.10
	5	6.25	6.25	6.25	13.77	13.77	13.77	8.86	8.86	12.65	12.65	28.66	28.66	30.86	30.86	9.11	9.11	5.12	5.12	19.10	19.10
	6	6.25	6.25	6.25	13.77	13.77	13.77	8.86	8.86	12.65	12.65	28.66	28.66	30.86	30.86	9.11	9.11	5.12	5.12	19.10	19.10
#3	**7**	7.46	7.46	7.46	9.60	9.60	9.60	4.89	4.89	14.70	14.70	33.22	33.22	27.47	27.47	4.80	4.80	3.60	3.60	18.03	18.03
	8	7.46	7.46	7.46	9.60	9.60	9.60	4.89	4.89	14.70	14.70	33.22	33.22	27.47	27.47	4.80	4.80	3.60	3.60	18.03	18.03
	9	7.46	7.46	7.46	9.60	9.60	9.60	4.89	4.89	14.70	14.70	33.22	33.22	27.47	27.47	4.80	4.80	3.60	3.60	18.03	18.03
#4	**10**	5.25	5.25	5.25	7.86	7.86	7.86	2.92	2.92	12.91	12.91	34.58	34.58	29.35	29.35	3.01	3.01	5.66	5.66	20.24	20.24
	11	5.25	5.25	5.25	7.86	7.86	7.86	2.92	2.92	12.91	12.91	34.58	34.58	29.35	29.35	3.01	3.01	5.66	5.66	20.24	20.24
	12	5.25	5.25	5.25	7.86	7.86	7.86	2.92	2.92	12.91	12.91	34.58	34.58	29.35	29.35	3.01	3.01	5.66	5.66	20.24	20.24

(*continued on next page*)

Table A.17 (*continued*).

Line	Buses	Charging station option $j \in \mathcal{N}$																			
		1	2	3	4	5	6	7	8	9	10	11	12	13	14	15	16	17	18	19	20
	13	15.20	15.20	15.20	22.90	22.90	22.90	17.94	17.94	19.69	19.69	19.48	19.48	31.30	31.30	18.11	18.11	10.99	10.99	17.01	17.01
#5	**14**	15.20	15.20	15.20	22.90	22.90	22.90	17.94	17.94	19.69	19.69	19.48	19.48	31.30	31.30	18.11	18.11	10.99	10.99	17.01	17.01
	15	15.20	15.20	15.20	22.90	22.90	22.90	17.94	17.94	19.69	19.69	19.48	19.48	31.30	31.30	18.11	18.11	10.99	10.99	17.01	17.01
	16	15.72	15.72	15.72	23.44	23.44	23.44	18.47	18.47	20.51	20.51	18.98	18.98	30.85	30.85	18.62	18.62	11.28	11.28	16.46	16.46
#6	**17**	15.72	15.72	15.72	23.44	23.44	23.44	18.47	18.47	20.51	20.51	18.98	18.98	30.85	30.85	18.62	18.62	11.28	11.28	16.46	16.46
	18	15.72	15.72	15.72	23.44	23.44	23.44	18.47	18.47	20.51	20.51	18.98	18.98	30.85	30.85	18.62	18.62	11.28	11.28	16.46	16.46
	19	5.44	5.44	5.44	9.41	9.41	9.41	5.69	5.69	17.12	17.12	34.83	34.83	25.19	25.19	5.32	5.32	4.78	4.78	17.01	17.01
#7	**20**	5.44	5.44	5.44	9.41	9.41	9.41	5.69	5.69	17.12	17.12	34.83	34.83	25.19	25.19	5.32	5.32	4.78	4.78	17.01	17.01
	21	5.44	5.44	5.44	9.41	9.41	9.41	5.69	5.69	17.12	17.12	34.83	34.83	25.19	25.19	5.32	5.32	4.78	4.78	17.01	17.01
	22	6.50	6.50	6.50	9.42	9.42	9.42	5.73	5.73	17.18	17.18	34.86	34.86	25.14	25.14	5.35	5.35	4.82	4.82	16.99	16.99
#8	**23**	6.50	6.50	6.50	9.42	9.42	9.42	5.73	5.73	17.18	17.18	34.86	34.86	25.14	25.14	5.35	5.35	4.82	4.82	16.99	16.99
	24	6.50	6.50	6.50	9.42	9.42	9.42	5.73	5.73	17.18	17.18	34.86	34.86	25.14	25.14	5.35	5.35	4.82	4.82	16.99	16.99
	25	6.02	6.02	6.02	12.26	12.26	12.26	8.08	8.08	18.15	18.15	32.11	32.11	24.08	24.08	7.83	7.83	8.56	8.56	14.52	14.52
#9	**26**	6.02	6.02	6.02	12.26	12.26	12.26	8.08	8.08	18.15	18.15	32.11	32.11	24.08	24.08	7.83	7.83	8.56	8.56	14.52	14.52
	27	6.02	6.02	6.02	12.26	12.26	12.26	8.08	8.08	18.15	18.15	32.11	32.11	24.08	24.08	7.83	7.83	8.56	8.56	14.52	14.52
	28	6.37	6.37	6.37	13.90	13.90	13.90	8.98	8.98	12.74	12.74	28.54	28.54	30.83	30.83	9.23	9.23	5.12	5.12	19.03	19.03
#10	**29**	6.37	6.37	6.37	13.90	13.90	13.90	8.98	8.98	12.74	12.74	28.54	28.54	30.83	30.83	9.23	9.23	5.12	5.12	19.03	19.03
	30	6.37	6.37	6.37	13.90	13.90	13.90	8.98	8.98	12.74	12.74	28.54	28.54	30.83	30.83	9.23	9.23	5.12	5.12	19.03	19.03

Table A.18
Charging start (f_{kj}) and end (l_{kj}) time values of each electric bus $k \in \mathcal{K}$ (3 electric buses per bus line) at the assigned charging location $j \in \mathcal{N}$ across all β (%) variations (in minutes past midnight) – Athens case study network.

Lines	Buses	β (%) percentage variations									
		100 (%)		95 (%)		80 (%)		75 (%)		60 (%)	
		f_{kj}	l_{kj}	f_{kj}	l_{kj}	f_{kj}	l_{kj}	f_{kj}	l_{kj}	f_{kj}	l_{kj}
	1	759.75	777.16	749.48	766.86	732.73	750.14	729.80	747.04	720.55	737.74
#1	**2**	797.19	808.10	776.21	793.63	756.95	773.71	755.70	772.44	748.85	765.54
	3	846.85	866.26	841.71	861.66	815.16	834.45	812.10	831.34	803.13	822.31
	4	914.15	933.28	893.61	913.41	870.24	889.03	871.29	890.66	859.09	877.81
#2	**5**	909.17	989.67	905.84	986.13	889.05	908.76	885.96	905.54	876.50	896
	6	764.18	780.81	717.99	734.27	705.73	770.87	700.14	764.45	692.90	708.90
	7	925.52	1004.61	900.59	919.70	891.55	910.61	888.68	907.70	880.04	899.02
#3	**8**	890.82	907.96	861.66	878.77	837.97	906.45	834.36	851.38	825.20	893.12
	9	838.98	857.62	823.09	841.71	805.15	823.69	802.83	876.91	797.55	871.47
	10	956.17	976.24	945.14	965.21	934.86	954.91	930.43	950.49	923.58	1003.78
#4	**11**	856.26	924.52	837.59	905.84	822.21	890.43	817.20	834.26	810.21	827.27
	12	956.03	1020.29	965.21	981.27	921.69	985.95	919.71	983.92	911.12	927.17
	13	867.46	885.31	843.73	861.50	835.13	853.42	827.04	896.29	818.99	887.56
#5	**14**	935.71	958.06	919.70	943.02	908.76	930.64	896.29	983.54	887.73	974.30
	15	867.85	955.27	861.50	883.25	840	861.85	845.34	868.12	828.36	849.50
	16	871.74	890.82	857.01	928.35	845.65	915.42	841.46	858.84	841.02	859.09
#6	**17**	914.23	935.17	884.32	905.16	869.90	891.30	861.02	881.39	849.50	869.71
	18	1062.88	1152.61	1053.48	1142.81	1037.93	1059.90	1034.65	1056.52	1024.63	1046.33
	19	1035.90	1054.55	1024.91	1099.37	1013.09	1031.63	1009.59	1084.07	1000.53	1018.90
#7	**20**	918.03	935.51	906.79	975.25	890.54	959.16	885.28	953.02	875.11	942.58
	21	1023.09	1095.71	1010.37	1028.49	996.91	1014.87	992.46	1010.39	985.19	1056.66
	22	1121.30	1159.97	1104.29	1114.13	1089.09	1098.56	1087.88	1097.51	1079.78	1096.65
#8	**23**	1022.40	1038.65	1002.70	1018.92	984.41	1048.30	980.90	1044.69	971.30	987.18
	24	1107.22	1119.61	1057.77	1136.29	1046.71	1125.26	1043.91	1121.70	1036.23	1055.61
	25	1163.29	1207.96	1153.40	1164.54	1139.10	1183.32	1135.94	1146.98	1128.07	1139.07
#9	**26**	988.98	1007.64	984.06	1002.70	974.52	993.19	969.19	987.73	958.95	977.45
	27	1135.65	1144.32	1129.52	1138.17	1116.39	1125.04	1115.94	1150.10	1105.20	1113.70
	28	1089.72	1100.05	1067.71	1085.50	1048.19	1118.62	1045.63	1115.94	1038.78	1108.78
#10	**29**	1249.11	1288.44	1220.04	1259.18	1198.50	1237.64	1196.27	1234.58	1188.33	1197.83
	30	1157.45	1168.28	1140.11	1150.89	1130.56	1141.39	1128.67	1139.51	1122.06	1132.80

Table A.19
Remaining State of Charge of each electric bus $k \in \mathcal{K}$ upon their arrival at the charging location $j \in \mathcal{N}$ across all β (%) variations (kWh) – Athens case study network.

	β % percentage variations				
Buses	100 (%)	95 (%)	80 (%)	75 (%)	60 (%)
1	30.18	30.24	30.18	30.52	30.63
2	31.18	30.16	31.48	31.52	31.63
3	26.18	25.11	26.42	26.52	26.63
4	26.75	25.40	27.43	26.27	27.56
5	24.75	24.86	25.57	25.84	26.00
6	31.75	32.43	32.43	32.85	33.00
7	25.46	26.76	26.87	26.96	27.04
8	30.72	30.76	30.76	30.96	31.04
9	27.72	27.76	27.91	27.96	28.04
10	24.87	24.87	24.88	24.88	24.90
11	30.87	30.87	30.89	30.88	30.88
12	32.87	32.87	32.87	32.90	32.89
13	29.29	29.46	28.43	30.37	30.71
14	20.29	20.36	21.25	21.38	21.71
15	21.29	21.48	21.29	20.01	22.71
16	26.83	29.33	30.12	30.25	28.87
17	23.13	23.33	22.20	24.25	24.59
18	20.14	20.33	21.08	21.25	21.59
19	27.69	27.77	27.93	27.76	28.27
20	30.04	30.77	30.69	31.13	31.27
21	28.69	28.77	29.08	29.13	29.27
22	30.66	30.31	31.05	30.75	31.24
23	32.49	32.57	33.05	33.11	33.24
24	25.21	25.74	25.73	26.10	26.24
25	27.67	27.71	27.89	27.92	28.00
26	27.67	27.71	27.67	27.92	28.00
27	32.67	32.71	32.69	32.92	33.00
28	29.34	29.43	29.79	29.84	30.00
29	30.34	30.43	30.43	30.84	31.00
30	28.34	28.43	28.34	28.32	28.51

Table A.20
Active service time, idle time due to deadheading and charging, and downtime (%) for each electric bus $k \in \mathcal{K}$ (3 electric buses per bus line) under the stochastic approach (in minutes) – Athens case study network.

Lines	Buses	Active service time	Idle time due to deadheading	Idle time due to charging	Bus downtime (%)
#1	**1**	438.90	10.85	17.41	6.05%
	2	450.45	10.74	16.91	5.78%
	3	484.40	12.45	19.41	6.17%
#2	**4**	553.89	10.26	19.13	5.04%
	5	534.44	9.72	80.51	14.44%
	6	422.76	11.43	16.63	6.22%
#3	**7**	697.62	12.90	79.09	11.65%
	8	514.96	9.27	17.14	4.88%
	9	498.96	10.02	18.64	5.43%
#4	**10**	570.74	5.43	20.07	4.28%
	11	535.82	5.44	68.26	12.09%
	12	605.61	5.42	64.26	10.32%
#5	**13**	484.98	17.47	17.86	6.79%
	14	462.16	18.55	22.36	8.13%
	15	439.73	18.11	87.42	19.35%
#6	**16**	504.03	27.70	19.09	8.49%
	17	526.24	18.00	20.93	6.89%
	18	647.96	19.92	89.73	14.47%

(*continued on next page*)

Table A.20 (*continued*).

Lines	Buses	Active service time	Idle time due to deadheading	Idle time due to charging	Bus downtime (%)
	19	698.23	7.67	18.65	3.63%
#7	**20**	608.08	9.95	17.48	4.32%
	21	700.55	7.54	72.62	10.27%
	22	677.18	9.12	38.68	6.59%
#8	**23**	606.70	10.70	16.25	4.25%
	24	677.45	9.77	12.39	3.17%
	25	778.36	9.93	44.67	6.55%
#9	**26**	663.88	10.10	18.67	4.15%
	27	779.75	10.90	8.67	2.45%
	28	721.36	8.35	10.33	2.52%
#10	**29**	819.71	9.40	39.33	5.61%
	30	758.83	8.61	10.83	2.50%

References

Abel, G., 2024. VDI / YUTONG. Technical Report, Sydney Business Scool, URL: https://business.sydney.edu.au/_data/assets/pdf_file/0010/514576/Greg-Abel_without-videos.pdf.

An, K., 2020. Battery electric bus infrastructure planning under demand uncertainty. Transp. Res. C 111, 572–587. http://dx.doi.org/10.1016/j.trc.2020.01.009.

Basma, H., Mansour, C., Haddad, M., Nemer, M., Stabat, P., 2023. A novel method for co-optimizing battery sizing and charging strategy of battery electric bus fleets: An application to the city of paris. Energy 285, 129459.

Cheshmehzangi, A., Chen, H., 2021. China's Sustainability Transitions: Low Carbon and Climate-Resilient Plan for Carbon Neutral 2060. Springer Nature.

Deb, S., Tammi, K., Gao, X.Z., Kalita, K., Mahanta, P., Cross, S., 2022. A robust two-stage planning model for the charging station placement problem considering road traffic uncertainty. IEEE Trans. Intell. Transp. Syst. 23, 6571–6585. http://dx.doi.org/10.1109/TITS.2021.3058419.

El Faouzi, N., Maurin, M., 2007. Reliability of travel time under log-normal distribution: methodological issues and path travel time confidence derivation. In: Transportation Research Board 86th Annual Meeting (CD-ROM). Transportation Research Record. Washington, DC.

Elavarasan, R.M., Pugazhendhi, R., Irfan, M., Mihet-Popa, L., Khan, I.A., Campana, P.E., 2022. State-of-the-art sustainable approaches for deeper decarbonization in europe–an endowment to climate neutral vision. Renew. Sustain. Energy Rev. 159, 112204.

Esmaeilnejad, S., Kattan, L., Wirasinghe, S., 2023. Optimal charging station locations and durations for a transit route with battery-electric buses: A two-stage stochastic programming approach with consideration of weather conditions. Transp. Res. C 156, 104327. http://dx.doi.org/10.1016/j.trc.2023.104327.

Eurostat, 2024. Greenhouse gas emission statistics - emission inventories. https://ec.europa.eu/eurostat/statistics-explained/index.php?title=Greenhouse_gas_emission_statistics_-_emission_inventories. (Accessed 30 August 2024).

Gkiotsalitis, K., 2021. Improving service regularity for high-frequency bus services with rescheduling and bus holding. J. Traffic Transp. Eng. (Engl. Ed.) 8, 778–794.

Gkiotsalitis, K., 2023. Operational planning and control. In: Public Transport Optimization. Springer, pp. 545–587.

Gkiotsalitis, K., Cats, O., Liu, T., Bult, J., 2023a. An exact optimization method for coordinating the arrival times of urban rail lines at a common corridor. Transp. Res. E: Logist. Transp. Rev. 178, 103265.

Gkiotsalitis, K., Iliopoulou, C., Kepaptsoglou, K., 2023b. An exact approach for the multi-depot electric bus scheduling problem with time windows. European J. Oper. Res. 306, 189–206.

Gkiotsalitis, K., Schmidt, M., van der Hurk, E., 2022. Subline frequency setting for autonomous minibusses under demand uncertainty. Transp. Res. C 135, 103492.

He, Y., Liu, Z., Zhang, Y., Song, Z., 2023. Time-dependent electric bus and charging station deployment problem. Energy 128227.

He, Y., Song, Z., Liu, Z., 2019. Fast-charging station deployment for battery electric bus systems considering electricity demand charges. Sustain. Cities Soc. 48, 101530.

Horrox, J., Casale, M., 2019. Electric buses in america: Lessons from cities pioneering clean transportation. US PIRG Education Fund. (Accessed 6 June 2021).

Hsu, Y.T., Yan, S., Huang, P., 2021. The depot and charging facility location problem for electrifying urban bus services. Transp. Res. D 100, 103053.

Hu, H., Du, B., Liu, W., Perez, P., 2022. A joint optimisation model for charger locating and electric bus charging scheduling considering opportunity fast charging and uncertainties. Transp. Res. C 141, 103732. http://dx.doi.org/10.1016/j.trc.2022.103732.

Huang, L., Chen, X., Huo, W., Wang, J., Zhang, F., Bai, B., Shi, L., 2021. Branch and bound in mixed integer linear programming problems: A survey of techniques and trends. arXiv preprint arXiv:2111.06257.

International Energy Agency, 2024. Transport. URL: https://www.iea.org/energy-system/transport. (Accessed 30 July 2024).

Kchaou-Boujelben, M., 2021. Charging station location problem: A comprehensive review on models and solution approaches. Transp. Res. C 132, 103376.

Kim, S., Pasupathy, R., Henderson, S.G., 2015. A guide to sample average approximation. In: Handbook of Simulation Optimization. pp. 207–243.

Kunith, A., Mendelevitch, R., Goehlich, D., 2017. Electrification of a city bus network—an optimization model for cost-effective placing of charging infrastructure and battery sizing of fast-charging electric bus systems. Int. J. Sustain. Transp. 11, 707–720.

Lim, L.K., Ab Muis, Z., Hashim, H., Ho, W.S., Idris, M.N.M., 2021. Potential of electric bus as a carbon mitigation strategies and energy modelling: a review. Chem. Eng. Trans. 89, 529–534.

Liu, K., Gao, H., Wang, Y., Feng, T., Li, C., 2022. Robust charging strategies for electric bus fleets under energy consumption uncertainty. Transp. Res. D 104, 103215.

Liu, Y., Liang, H., 2021. A three-layer stochastic energy management approach for electric bus transit centers with pv and energy storage systems. IEEE Trans. Smart Grid 12, 1346–1357. http://dx.doi.org/10.1109/TSG.2020.3024148.

Liu, Z., Song, Z., He, Y., 2018. Planning of fast-charging stations for a battery electric bus system under energy consumption uncertainty. Transp. Res. Rec. 2672, 96–107.

Lotfi, M., Pereira, P., Paterakis, N., Gabbar, H.A., Catalão, J.P., 2020. Optimizing charging infrastructures of electric bus routes to minimize total ownership cost. In: 2020 IEEE International Conference on Environment and Electrical Engineering and 2020 IEEE Industrial and Commercial Power Systems Europe. EEEIC/I & CPS Europe, IEEE, pp. 1–6.

Mazloumi, E., Currie, G., Rose, G., 2010. Using gps data to gain insight into public transport travel time variability. J. Transp. Eng. 136, 623–631.

Morrison, D.R., Jacobson, S.H., Sauppe, J.J., Sewell, E.C., 2016. Branch-and-bound algorithms: A survey of recent advances in searching, branching, and pruning. Discrete Optim. 19, 79–102.

Olsen, N., Kliewer, N., 2022. Location planning of charging stations for electric buses in public transport considering vehicle scheduling: A variable neighborhood search based approach. Appl. Sci. 12 (3855), http://dx.doi.org/10.3390/app12083855.

Plessmann, G., Blechinger, P., 2017. How to meet eu ghg emission reduction targets? a model based decarbonization pathway for Europe's electricity supply system until 2050. Energy Strat. Rev. 15, 19–32.

Qi, Z., Yang, J., Jia, R., Wang, F., 2018. Investigating real-world energy consumption of electric vehicles: a case study of shanghai. Procedia Comput. Sci. 131, 367–376.

Rahman, M.M., Wirasinghe, S., Kattan, L., 2018. Analysis of bus travel time distributions for varying horizons and real-time applications. Transp. Res. C 86, 453–466.

Randhahn, A., Knote, T., 2020. Deployment of charging infrastructure for battery electric buses. In: Towards User-Centric Transport in Europe 2: Enablers of Inclusive, Seamless and Sustainable Mobility. pp. 169–183.

Rigogiannis, N., Bogatsis, I., Pechlivanis, C., Kyritsis, A., Papanikolaou, N., 2023. Moving towards greener road transportation: A review. Clean Technol. 5, 766–790.

Shahid, S., Minhans, A., Puan, O.C., 2014. Assessment of greenhouse gas emission reduction measures in transportation sector of Malaysia. J. Teknol. 70.

Shao, S., Tan, Z., Liu, Z., Shang, W., 2022. Balancing the ghg emissions and operational costs for a mixed fleet of electric buses and diesel buses. Appl. Energy 328, 120188.

Singh, R., Graham, D.J., Trompet, M., Barry, J., 2024. A sampling scheme for quantifying and benchmarking on time performance of urban bus transit. Transp. Res. A 180, 103945.

Teoh, L.E., Khoo, H.L., Goh, S.Y., Chong, L., 2017. Scenario-based electric bus operation: A case study of putrajaya, Malaysia. Int. J. Transp. Sci. Technol. 7, http://dx.doi.org/10.1016/j.ijtst.2017.09.002.

Thorne, R.J., Hovi, I.B., Figenbaum, E., Pinchasik, D.R., Amundsen, A.H., Hagman, R., 2021. Facilitating adoption of electric buses through policy: Learnings from a trial in norway. Energy Policy 155, 112310.

Tzamakos, D., Iliopoulou, C., Kepaptsoglou, K., 2022. Electric bus charging station location optimization considering queues. Int. J. Transp. Sci. Technol. 12, http://dx.doi.org/10.1016/j.ijtst.2022.02.007.

United Nations Economic and Social Commission for Asia and the Pacific (ESCAP), 2024. Accelerating electric mobility in public transport. URL: https://repository.unescap.org/bitstream/handle/20.500.12870/6756/ESCAP-2024-PB-TD-Accelerating-Electric-Mobility-in-Public-Transport.pdf?sequence=1&isAllowed=y.

U.S. Environmental Protection Agency, 2024. Sources of greenhouse gas emissions. https://www.epa.gov/ghgemissions/sources-greenhouse-gas-emissions. (Accessed 30 August 2024).

Uslu, T., Kaya, O., 2021. Location and capacity decisions for electric bus charging stations considering waiting times. Transp. Res. D 90, 102645.

Voigt, C., Lamprecht, R.E., Marushchak, M.E., Lind, S.E., Novakovskiy, A., Aurela, M., Martikainen, P.J., Biasi, C., 2017. Warming of subarctic tundra increases emissions of all three important greenhouse gases–carbon dioxide, methane, and nitrous oxide. Global Change Biol. 23, 3121–3138.

Wang, Y., Dong, W., Zhang, L., Chin, D., Papageorgiou, M., Rose, G., Young, W., 2012. Speed modeling and travel time estimation based on truncated normal and lognormal distributions. Transp. Res. Rec. 2315, 66–72.

Wang, X., Song, Z., Xu, H., Wang, H., 2023. En-route fast charging infrastructure planning and scheduling for battery electric bus systems. Transp. Res. D 117, 103659.

Wu, X., Feng, Q., Bai, C., Lai, C.S., Jia, Y., Lai, L.L., 2021. A novel fast-charging stations locational planning model for electric bus transit system. Energy 224, 120106.

Wu, X., Freese, D., Cabrera, A., Kitch, W.A., 2015. Electric vehicles' energy consumption measurement and estimation. Transp. Res. D 34, 52–67.

Zghidi, I., Hnich, B., Rebaï, A., 2018. Modeling uncertainties with chance constraints. Constraints 23, 196–209.

Zhou, Y., Ong, G., Meng, Q., Cui, H., 2023. Electric bus charging facility planning with uncertainties: Model formulation and algorithm design. Transp. Res. C 150, 104108. http://dx.doi.org/10.1016/j.trc.2023.104108.